

Low-ground/High ground capacity regions analysis for Bosonic Gaussian Channels

Farzad Kianvash,^{1,*} Marco Fanizza,^{2,1} and Vittorio Giovannetti¹

¹*NEST, Scuola Normale Superiore and Istituto Nanoscienze-CNR, I-56126 Pisa, Italy*

²*Física Teòrica: Informació i Fenòmens Quàntics, Departament de Física,
Universitat Autònoma de Barcelona, ES-08193 Bellaterra (Barcelona), Spain.*

(Dated: September 27, 2024)

We present a comprehensive characterization of the interconnections between single-mode, phase-insensitive Gaussian Bosonic Channels resulting from channel concatenation. This characterization enables us to identify, in the parameter space of these maps, two distinct regions: low-ground and high-ground. In the low-ground region, the information capacities are smaller than a designated reference value, while in the high-ground region, they are provably greater. As a direct consequence, we systematically outline an explicit set of upper bounds for the quantum and private capacity of these maps, which combine known upper bounds and composition rules, improving upon existing results.

PACS numbers: 03.67.-a, 03.67.Ac, 03.65.Ta.

I. INTRODUCTION

The efficiency of classical communication lines can be expressed using a single, simple formula [1, 2]. However, when it comes to quantum communication lines (quantum channels) that utilize quantum systems as information carriers instead of classical signals [3–6], this simplification no longer holds. Instead, a multitude of different and computationally challenging capacity functionals are required to fully assess the quality of these transmission lines. For instance, the classical capacity of a quantum channel, characterizes the optimal rate of classical bits that can be reliably transferred per channel uses; the quantum capacity instead provides the optimal rate of transmitted qubits, and the private capacity, the optimal rate of bits that can be transmitted privately along the channel. In our study, we specifically focus on a special class of quantum communication lines known as Gaussian Bosonic Channels (GBCs), which are commonly employed to model communication procedures utilizing the electromagnetic field as the carrier of transmitted messages [7–10]. Despite significant progress made in recent years, the analysis of GBCs still presents complex challenges. Specifically, computing the exact values of certain information capacities for these maps requires optimization techniques that remain difficult to tackle. In principle, calculating these quantities necessitates taking the limit of properly regularized entropic functionals, considering the potential utilization of entanglement across multiple channel uses [11–29]. Given these complexities, the derivation of upper and lower bounds for the capacities of significant channels represents crucial progress in the field.

An established strategy for upper bounding information capacities involves utilizing data processing inequalities. For instance, it is possible to obtain an upper bound

for the capacity of a specific channel by expressing it as a concatenation of channels whose capacities are already known or upper bounded [30–41]. In this article, we employ this method to enhance the previously established bounds in the literature [39–42] for the quantum and private capacity of single-mode, phase-insensitive Gaussian Bosonic Channels (PI-GBCs). To achieve this result, we present a detailed decomposition of the parameter space of PI-GBC maps into regions encompassing all channels that can simulate a given channel through concatenation with other PI-GBC elements.

The structure of the article is as follows: In Sec. II we introduce the fundamental concepts and notation used in this article. We start by giving an overview of continuous variable quantum channels and establish crucial notation. Then, we briefly discuss various quantum capacities of a quantum channel, namely quantum capacity, private capacity, two-way quantum capacity, and secret-key capacity. Following that, we introduce phase-insensitive one-mode GBCs and establish specific notation to aid us throughout the manuscript. In Sec. III we provide a concise review of the current state-of-the-art bounds for the quantum capacity of GBCs. We discuss the main techniques used to derive these bounds, including the use of data processing inequalities and channel concatenation. We also highlight the key challenges that remain in computing the exact quantum capacity for these channels. In Sec. IV we study the parameter space of PI-GBCs in terms of channel concatenation. We present a detailed decomposition of the parameter space of PI-GBC maps into regions encompassing all channels that can simulate a given channel through concatenation with other PI-GBC elements. This analysis allows us to identify the channels that can be used to upper bound the quantum capacity of a given PI-GBC. In Sec. VI we derive new upper bounds for the quantum and private capacity of single-mode, phase-insensitive Gaussian Bosonic Channels (PI-GBCs) by employing the channel concatenation method discussed in Sec. IV. We demonstrate that our new bounds improve upon the previously established

*Electronic address: farzad.kianvash@sns.it

bounds in the literature, providing a more accurate estimation of the capacities for these channels. Sec. VII concludes the manuscript.

II. PRELIMINARIES

A quantum communication line connecting two distant parties can be seen as a physical transformation that associates the states of a system A , representing the input messages of the model, with the states of a second system B , representing the associated output messages. At mathematical level such an object is described as a completely positive trace preserving (LCPTP) linear map $\Lambda : \mathcal{B}_1(\mathcal{H}_A) \mapsto \mathcal{B}_1(\mathcal{H}_B)$ that links the set of the trace-class operators of the (possibly infinite dimensional) Hilbert spaces $\mathcal{H}_A, \mathcal{H}_B$ associated with A and B respectively [5, 6]. By Stinespring representation we can always express Λ as a reduction of an isometry \hat{V} that connects \mathcal{H}_A to an extension \mathcal{H}_{BE} of \mathcal{H}_B , i.e. $\Lambda(\cdots) = \text{Tr}_E(\hat{V} \cdots \hat{V}^\dagger)$, with Tr_E being the partial trace with respect to E . Such a construction allows us to introduce the notion of complementary channel $\tilde{\Lambda} : \mathcal{B}_1(\mathcal{H}_A) \mapsto \mathcal{B}_1(\mathcal{H}_E)$ defined as $\tilde{\Lambda}(\cdots) := \text{Tr}_B(\hat{V} \cdots \hat{V}^\dagger)$, which can be interpreted as the transformation induced on the environment of the communication line by the signaling process [43].

Similarly to what happens in classical information theory, the efficiency of a quantum channel Λ can be gauged in terms of a series figures of merit (the quantum capacities of the channel) that evaluate the optimal ratio between the amount of data which can be sent reliably through the channel and the total amount of redundancy needed to achieve such a goal [3–6]. In this paper we focus on special instances of such quantities which in the context of continuous variable quantum information processing (see next section), admit optimal finite values even when allowing unbounded energy resources, i.e. the quantum capacity $Q(\Lambda)$, the private capacity $P(\Lambda)$, the two-way quantum capacity $Q_2(\Lambda)$, and the secret-key capacity $K(\Lambda)$ [6]. They are hierarchically ordered via the inequalities

$$K(\Lambda) \geq Q_2(\Lambda), P(\Lambda) \geq Q(\Lambda). \quad (1)$$

The smallest among such terms, i.e. $Q(\Lambda)$, measures the maximum rate at which the communication line can transmit quantum information reliably over asymptotically many uses of the channel [11–13]; $P(\Lambda)$ is instead the maximum rate at which we can transmit classical messages through the channel Λ in such a way that an external party that is monitoring the line, will not be able to read such messages [13]; $Q_2(\Lambda)$ represents the maximum quantum information transmission rate attainable by allowing the communicating party to use (arbitrary) distillation protocols through the use of a classical side-channel [44]; and finally the largest of these quantities, i.e. $K(\Lambda)$, describes the maximum rate at which two parties can use the channel to distill secret random string of bits.

Despite being operationally well defined, no universal formula is known that allows one to explicitly compute the values of $Q_2(\Lambda)$ and $K(\Lambda)$ as entropic functionals. On the contrary, such characterizations exist for $Q(\Lambda)$ and for $P(\Lambda)$, based on regularized optimizations of, respectively, the output coherent information for Q , and the Holevo information gap between Λ and its complementary map $\tilde{\Lambda}$, for P . Even in these cases, however, the explicit computation of $Q(\Lambda)$ and $P(\Lambda)$ is typically rather challenging and has been carried out only a very limited set of models (in particular for the special classes of degradable and anti-degradable maps). A possible way to circumvent this problem is to make use of data-processing inequalities. Specifically a simple resource counting argument can be invoked to observe that, if a quantum channel Λ can be expressed in terms of a LCPTP map Λ' via the concatenated action of other two LCPTP linear maps Λ_1, Λ_2 , then the following relations hold

$$\Lambda = \Lambda_2 \circ \Lambda' \circ \Lambda_1 \implies \mathcal{K}(\Lambda) \leq \mathcal{K}(\Lambda'), \quad (2)$$

where hereafter we shall use the symbol \mathcal{K} to represent an arbitrary capacity (e.g. Q, P, Q_2 , or K) see e.g. [4–6]. Accordingly if the capacity values of Λ_1 or Λ_2 are known, or if upper bounds for those quantities are available, we can then use (2) to constraint the performances of Λ . Alternatively, if instead the capacity of Λ is known or if a lower bound for it is available, we can use (2) to provide lower bounds for those of Λ_1 and Λ_2 . In what follows, we shall make use of this simple idea to improve the capacity analysis of a special class of quantum maps which plays an important role in quantum information theory, that is the Bosonic Gaussian Channels set, whose properties are briefly reviewed in the next subsection.

A. Bosonic Gaussian Channels

Bosonic Gaussian Channels (BGCs) model a vast collection of noise models that tamper communication schemes which rely on the uses of e.m. signals [4, 9]. Formally they can be introduced as a special set of LCPT transformations which act on the Hilbert space $L^2(\mathbb{R}^n)$ of the square integrable functions, representing the states of n independent harmonic oscillators each corresponding to an individual mode of the field. Indicating with $\hat{\mathbf{r}} := (\hat{x}_1, \hat{p}_1, \dots, \hat{x}_n, \hat{p}_n)^T$ the set of canonical position and momentum operators of the modes, the action of a BGC map can be assigned in terms of linear mappings they induce on the first and second canonical momenta of the quantum states $\hat{\rho} \in \mathfrak{S}(L^2(\mathbb{R}^n))$ of the model, i.e. the $2n$ -dimensional real vector $\mathbf{m} := \text{Tr}(\hat{\mathbf{r}}\hat{\rho})$ and the $2n \times 2n$ real matrix $V := \text{Tr}(\{(\hat{\mathbf{r}} - \mathbf{m}), (\hat{\mathbf{r}} - \mathbf{m})^T\}\hat{\rho})$.

For what it concerns the present work we shall limit the analysis to a special subset of single-mode ($n = 1$) Phase Insensitive GBCs (or PI-GBCs in brief) formed by the maps $\Phi_{x,M}$ characterized by two positive noise parameters $x, M \geq 0$, whose action on the system is fully

determined by the transformations

$$\begin{cases} \mathbf{m} \xrightarrow{\Phi_{x,M}} \mathbf{m}' = \sqrt{x} \mathbf{m}, \\ V \xrightarrow{\Phi_{x,M}} V' = xV + (2M + |1-x|)I_2, \end{cases} \quad (3)$$

with \mathbf{m}' and V' being respectively the first and second momenta of the output state $\Phi_{x,M}(\hat{\rho})$, and with I_2 the 2×2 identity matrix. For $x = \eta \in [0, 1]$, and $M = (1 - \eta)N$ with $N \geq 0$, the mapping (3) corresponds to the thermal attenuator channel $\mathcal{E}_{\eta,N}$ which describes the interaction of the a single-mode of the e.m. field with an external thermal reservoir with N mean photon number, mediated by a beam-splitter coupling of transmissivity η ; for $x = g \geq 1$ and $M = (g - 1)N$ with $N \geq 0$ instead, $\Phi_{x,M}$ reduces to a thermal amplifier $\mathcal{A}_{g,N}$ which describes the interaction with the input mode with a thermal bath of mean photon number N , through a two mode squeezing operator with gain parameter g ; finally for $x = 1$ and $M = N \geq 0$, $\Phi_{x,M}$ reduces to the the additive classical noise GBC \mathcal{N}_N , i.e.

$$\begin{cases} \mathcal{E}_{\eta,N} := \Phi_{x=\eta,M=(1-\eta)N}, & \eta \in [0, 1], N \geq 0, \\ \mathcal{N}_N := \Phi_{x=1,M=N}, & N \geq 0. \\ \mathcal{A}_{g,N} := \Phi_{x=g,M=(g-1)N}, & g \geq 1, N \geq 0. \end{cases} \quad (4)$$

It is easy to check that the maps $\Phi_{x,M}$ are closed under concatenation, specifically given $(x_1, M_1), (x_2, M_2) \in \mathbb{R}_+^2$ we have that

$$\Phi_{x_3, M_3} = \Phi_{x_2, M_2} \circ \Phi_{x_1, M_1}, \quad (5)$$

is also a channel of the model with noise parameters $(x_3, M_3) \in (\mathbb{R}^+)^2$ fulfilling the identities

$$\begin{cases} x_3 = x_2 x_1, \\ M_3 = M_2 + x_2 M_1 + \frac{|x_2 - 1| + x_2 |x_1 - 1| - |x_2 x_1 - 1|}{2}, \end{cases} \quad (6)$$

which we express in terms of attenuators and amplifiers in Table I.

III. A BRIEF REVIEW ON PI-GBC CAPACITIES

We start by recalling that for N sufficiently large the channels $\mathcal{E}_{\eta,N}$, \mathcal{N}_N , and $\mathcal{A}_{g,N}$ are Entanglement-Breaking (EB) [5, 9], specifically

$$\begin{cases} \mathcal{E}_{\eta,N} \equiv \text{EB} \iff \eta \in [0, 1], N \geq \frac{\eta}{1-\eta}, \\ \mathcal{N}_N \equiv \text{EB} \iff N \geq 1, \\ \mathcal{A}_{g,N} \equiv \text{EB} \iff g \geq 1, N \geq \frac{1}{g-1}. \end{cases} \quad (7)$$

In the notation (3) this translates into the condition

$$\Phi_{x,M} \equiv \text{EB} \iff (x, M) \in \mathbb{EB}, \quad (8)$$

with the set

$$\mathbb{EB} := \{(x, M) \in (\mathbb{R}^+)^2 : M \geq M_{\text{EB}}(x)\}, \quad (9)$$

defined by the threshold function

$$M_{\text{EB}}(x) := \min\{1, x\}, \quad (10)$$

(see Fig. 1). By construction EB maps have all zero capacity values, i.e.

$$(x, M) \in \mathbb{EB} \implies \mathcal{K}(\Phi_{x,M}) = 0, \quad (11)$$

with the implication that can be reversed for the two-way capacity and for the secret-key capacity [45], meaning that \mathbb{EB} corresponds to the largest parameter region for which Q_2 and K are null. The case of Q and P is different as it is known that these capacities nullify also for channels which do not belong to \mathbb{EB} . In particular one has that

$$\begin{cases} Q(\mathcal{E}_{\eta,N}) = P(\mathcal{E}_{\eta,N}) = 0, & \eta \in [0, 1], N \geq \frac{2\eta-1}{2(1-\eta)}, \\ Q(\mathcal{A}_{g,N}) = P(\mathcal{A}_{g,N}) = 0, & g \geq 1, N \geq \frac{1}{2(g-1)}, \end{cases} \quad (12)$$

or

$$(x, M) \in \mathbb{AD} \implies Q(\Phi_{x,M}) = P(\Phi_{x,M}) = 0, \quad (13)$$

with

$$\mathbb{AD} := \{(x, M) \in (\mathbb{R}^+)^2 : M \geq M_{\text{AD}}(x)\}, \quad (14)$$

$$M_{\text{AD}}(x) := \min\{x - 1/2, 1/2\}, \quad (15)$$

corresponding to the Anti-Degradability (AD) region for the single-model PI-GBCs [46–49] (see Fig. 1). Notice that at present it is still not clear whether or not \mathbb{AD} is the largest set where Q and/or P nullify. What it is known are the exact values of these quantities for the special cases where $M = 0$. Specifically in the case of the quantum and private capacities we have [50]

$$P(\Phi_{x,0}) = Q(\Phi_{x,0}) = \max\{0, \log_2 \frac{x}{|1-x|}\}, \quad (16)$$

while for the secret-key and two-way capacities it holds [42]

$$K(\Phi_{x,0}) = Q_2(\Phi_{x,0}) = \log_2 \left(\frac{\max\{1, x\}}{|1-x|} \right), \quad (17)$$

(notice that for amplifiers, i.e. $x \geq 1$, Eq. (16) and (17) coincide).

(C ₁)	$\mathcal{E}_{\eta_2, N_2} \circ \mathcal{E}_{\eta_1, N_1} = \mathcal{E}_{\eta_3, N_3}$	$\begin{cases} \eta_3 = \eta_2 \eta_1 \\ (1 - \eta_3)N_3 = (1 - \eta_2)N_2 + (1 - \eta_1)\eta_2 N_1 \end{cases}$
(C ₂)	$\mathcal{A}_{g_2, N_2} \circ \mathcal{A}_{g_1, N_1} = \mathcal{A}_{g_3, N_3}$	$\begin{cases} g_3 = g_2 g_1 \\ (g_3 - 1)N_3 = (g_2 - 1)N_2 + (g_1 - 1)g_2 N_1 \end{cases}$
(C _{3.1})	$\mathcal{E}_{\eta_2, N_2} \circ \mathcal{A}_{g_1, N_1} = \begin{cases} \mathcal{E}_{\eta_3, N_3} \\ \mathcal{A}_{g_3, N_3} \end{cases}$	$\begin{cases} \eta_3 = \eta_2 g_1 \\ (1 - \eta_3)(2N_3 + 1) = (1 - \eta_2)(2N_2 + 1) + (\eta_3 - \eta_2)(2N_1 + 1) \end{cases}$
(C _{3.2})		$\begin{cases} g_3 = \eta_2 g_1 \\ (g_3 - 1)(2N_3 + 1) = (1 - \eta_2)(2N_2 + 1) + (g_3 - \eta_2)(2N_1 + 1) \end{cases}$
(C _{4.1})	$\mathcal{A}_{g_2, N_2} \circ \mathcal{E}_{\eta_1, N_1} = \begin{cases} \mathcal{E}_{\eta_3, N_3} \\ \mathcal{A}_{g_3, N_3} \end{cases}$	$\begin{cases} \eta_3 = g_2 \eta_1 \\ (1 - \eta_3)(2N_3 + 1) = (g_2 - 1)(2N_2 + 1) + (g_2 - \eta_3)(2N_1 + 1) \end{cases}$
(C _{4.2})		$\begin{cases} g_3 = g_2 \eta_1 \\ (g_3 - 1)(2N_3 + 1) = (g_2 - 1)(2N_2 + 1) + (g_2 - g_3)(2N_1 + 1) \end{cases}$

TABLE I: Composition rules (5) and (6) expressed in terms of thermal attenuators and amplifiers via the identities (4).

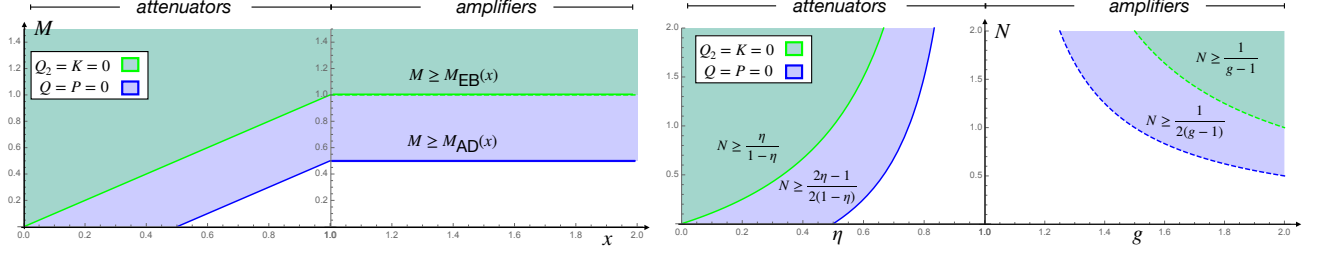


FIG. 1: Left panel: zero capacity regions for the PI-GBCs $\Phi_{x,M}$; Right panel: same plot expressed in terms of the parametrization (4). In both plots, the greenish areas represent the regions where the all the capacities (Q_2 , K , Q , and P) are zero. The bluish areas represent the region where Q and P are zero but Q_2 and K are not. Whether Q and P can be zero also for points in the white region is still an open problem.

A. Upper bounds

State-of-the-art upper bounds for the capacities of thermal attenuators and amplifiers are given in Refs. [39–42]. Specifically in [42] it has been showed that, outside the EB region (8), all the quantum capacities \mathcal{K} of thermal attenuators and amplifiers can be bounded as follows

$$\begin{cases} \mathcal{K}(\mathcal{E}_{\eta,N}) \leq \mathcal{K}_{\text{PLOB}}^{\text{att}}(\eta, N) := -h(N) - \log_2((1-\eta)\eta^N), \\ \mathcal{K}(\mathcal{A}_{g,N}) \leq \mathcal{K}_{\text{PLOB}}^{\text{amp}}(g, N) := -h(N) + \log_2\left(\frac{g^{N+1}}{g-1}\right), \end{cases} \quad (18)$$

with

$$h(x) := (x+1)\log_2(x+1) - x\log_2(x), \quad (19)$$

(see also Ref. [51] for a strong-converse extension of these inequalities). Partial improvements w.r.t. to the above inequalities for the case of quantum and private capacities, have been reported in Refs. [39, 40] where special instances of the decomposition rules (C_{3.1}) and (C_{3.2}) were employed to observe that outside the AD region (12) (i.e. for $N \leq \frac{2\eta-1}{2(1-\eta)}$ for $\mathcal{E}_{\eta,N}$ and $N \leq \frac{1}{2(g-1)}$ for $\mathcal{A}_{g,N}$) one can write $\mathcal{E}_{\eta,N} = \mathcal{E}_{\eta-N(1-\eta),0} \circ \mathcal{A}_{\frac{\eta}{\eta-N(1-\eta)},0}$

and $\mathcal{A}_{g,N} = \mathcal{E}_{1-(g-1)N,0} \circ \mathcal{A}_{\frac{g}{1-(g-1)N},0}$, which ultimately leads to

$$\begin{cases} Q(\mathcal{E}_{\eta,N}), P(\mathcal{E}_{\eta,N}) \leq Q(\mathcal{E}_{\eta-N(1-\eta),0}) = \log_2\left(\frac{\eta-N(1-\eta)}{1-\eta+N(1-\eta)}\right) \\ Q(\mathcal{A}_{g,N}), P(\mathcal{A}_{g,N}) \leq Q(\mathcal{E}_{1-(g-1)N,0}) = \log_2\left(\frac{1-(g-1)N}{(g-1)N}\right) \end{cases} \quad (20)$$

(notice that the bounds nullifies at the border with the AD region). In Ref. [41] instead, using degradable extensions of thermal attenuators, it was proven that

$$\begin{cases} Q(\mathcal{E}_{\eta,N}), P(\mathcal{E}_{\eta,N}) \leq Q_{\text{FKG}}^{\text{att}}(\eta, N), \\ Q(\mathcal{A}_{g,N}), P(\mathcal{A}_{g,N}) \leq Q_{\text{FKG}}^{\text{amp}}((g-1)N), \end{cases} \quad (21)$$

with

$$\begin{aligned} Q_{\text{FKG}}^{\text{att}}(\eta, N) &:= \log_2\left(\frac{\eta}{1-\eta}\right) + h((1-\eta)N) - h(\eta N), \\ Q_{\text{FKG}}^{\text{amp}}(M) &:= -\log_2(eM) + 2h\left(\frac{\sqrt{M^2+1}-1}{2}\right). \end{aligned}$$

Notice that the first is a function which, for fixed η is monotonically decreasing w.r.t. N and, for fixed N , monotonically increasing in η (being null for $\eta \leq 0.5$).

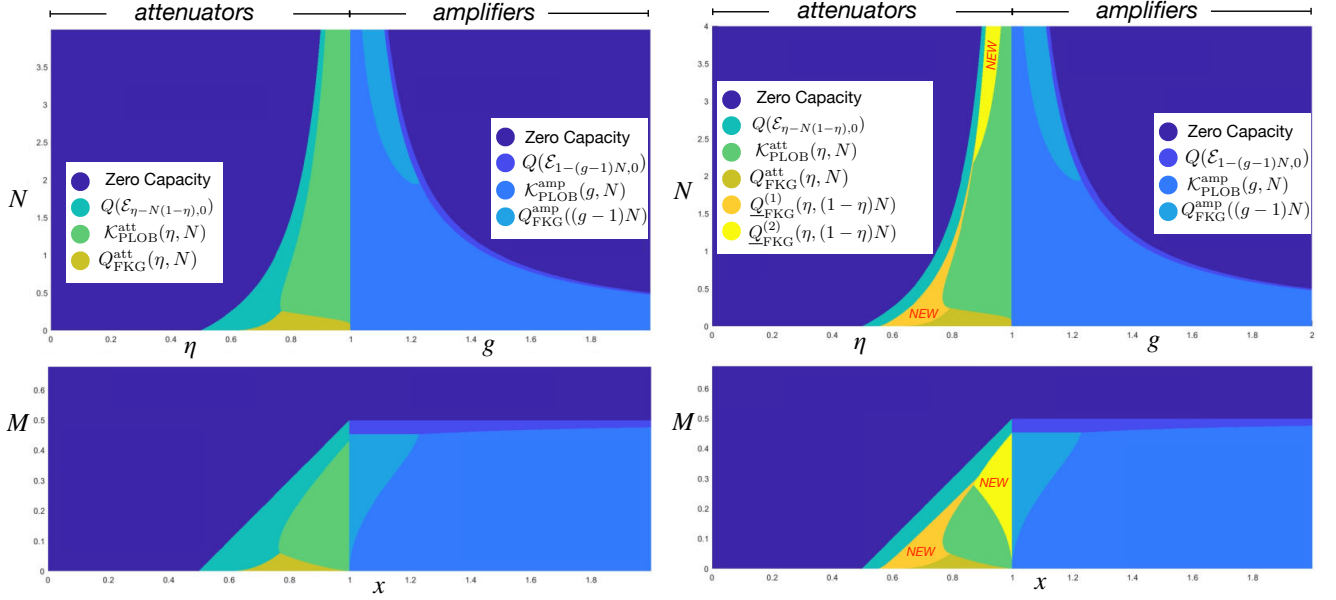


FIG. 2: **Left:** The top panel shows a numerical comparison between the upper bounds (18), (20), and (21) for the quantum capacity Q of the channels $\mathcal{E}_{\eta,N}$ and $\mathcal{A}_{g,N}$. Each region with different colour indicates which result is the best upper bound. Purple region is where the quantum capacity is zero according to Eq. (15). The bottom panel presents the same comparison expressed in terms of the x, M parametrization (3). **Right:** updated version of previous figure which includes the improved bounds $Q_{\text{FKG}}^{(1)}(x, M)$ and $Q_{\text{FKG}}^{(2)}(x, M)$ of Eq. (103): the orange and yellow regions (marked with the script *NEW*) are where they provide better constraints than the upper bounds of Sec. III A (notice that no improvement is obtained for amplifiers). The top panel reports the result in terms of the η, N and g, N parametrization, while the bottom panel reports the same result in the x, M parametrization.

On the contrary, for $M = (g-1)N \in [0, 1/2]$ (i.e. the only region where, in view of Eq. (12) it makes sense to consider (21)) $Q_{\text{FKG}}^{\text{amp}}(M)$ is a positive, monotonically increasing function. As explicitly shown in the left part of Fig. 2, one may notice that while for low values of η the upper bound (20) outperform the others, as η approaches 1, (18) and (21) win (in particular $Q_{\text{FKG}}^{\text{att}}$ provides the best bound in the low noise regime $N \ll 1$, while $Q_{\text{PLOB}}^{\text{att}}$ does it for higher N).

B. Lower bounds

Lower bounds for the two-way and secret capacities are provided by the inequalities [8, 52]

$$\begin{cases} K(\mathcal{E}_{\eta,N}) \geq Q_2(\mathcal{E}_{\eta,N}) \geq \max\{0, -h(N) - \log_2(1-\eta)\}, \\ K(\mathcal{A}_{g,N}) \geq Q_2(\mathcal{A}_{g,N}) \geq \max\{0, -h(N) + \log_2(\frac{g}{g-1})\}, \end{cases} \quad (22)$$

which have been improved in [45, 53]. [53] improved the lower bound for secret capacity adopting Gaussian protocols based on suitable trusted-noise detectors, and [45] showed that the region where Q_2 and K are non-zero extend beyond what predicted by the above equations, including all the non-EB region. A lower bound on Q and P is given instead by the coherent information for one use

of the channel, evaluated on an infinite temperature state

$$Q(\mathcal{E}_{\eta,N}) \geq Q_{\text{low}}^{\text{att}}(\eta, N) = \max\{0, \log_2(\frac{\eta}{1-\eta}) - h(N)\}. \quad (23)$$

IV. LOW GROUND/HIGH GROUND CAPACITY REGIONS ANALYSIS

Using the composition rules (5), (6) together with the data-processing inequality (2), in the parameter space of the maps (3) we can identify regions where the capacities are provably smaller or larger than an assigned reference value. For this purpose given $(x, M) \in (\mathbb{R}^+)^2$ we define $\mathbb{L}_{x,M} := \mathbb{L}(\Phi_{x,M})$ the collection of points $(x', M') \in (\mathbb{R}^+)^2$ such that the channel $\Phi_{x',M'}$ can be decomposed as a three-elements concatenation $\Phi_{x',M'} = \Phi_{\bar{x}_1, \bar{M}_1} \circ \Phi_{x,M} \circ \Phi_{\bar{x}_2, \bar{M}_2}$ that involves $\Phi_{x,M}$ together with two other maps $\Phi_{\bar{x}_1, \bar{M}_1}$ and $\Phi_{\bar{x}_2, \bar{M}_2}$, i.e. [54]

$$\mathbb{L}_{x,M} := \left\{ (x', M') \in (\mathbb{R}^+)^2 : \exists (\bar{x}_1, \bar{M}_1), (\bar{x}_2, \bar{M}_2) \in (\mathbb{R}^+)^2 \right. \\ \left. \Phi_{x',M'} = \Phi_{\bar{x}_1, \bar{M}_1} \circ \Phi_{x,M} \circ \Phi_{\bar{x}_2, \bar{M}_2} \right\}. \quad (24)$$

From (2) it turns out that

$$\mathcal{K}(\Phi_{x',M'}) \leq \mathcal{K}(\Phi_{x,M}), \quad \forall (x', M') \in \mathbb{L}_{x,M}. \quad (25)$$

so we dub $\mathbb{L}_{x,M}$ the *low-ground capacity region* of the channel $\Phi_{x,M}$. Notice in particular that, since $\Phi_{0,M'} \circ \Phi_{x,M} = \Phi_{0,M'}$ for all (x,M) and $M' \geq 0$, one has that all the points $(0,M')$ are included into $\mathbb{L}_{x,M}$, i.e.

$$(0, M') \in \mathbb{L}_{x,M}, \quad \forall M' \geq 0, \forall (x, M) \in (\mathbb{R}^+)^2. \quad (26)$$

By reversing the ordering of the concatenations in Eq. (24) we also introduce the *high-ground capacity region* $\mathbb{H}_{x,M} := \mathbb{H}(\Phi_{x,M})$ of the channel $\Phi_{x,M}$, i.e.

$$\mathbb{H}_{x,M} := \left\{ (x', M') \in (\mathbb{R}^+)^2 : \exists (\bar{x}_1, \bar{M}_1), (\bar{x}_2, \bar{M}_2) \in (\mathbb{R}^+)^2 \right. \\ \left. \Phi_{x,M} = \Phi_{\bar{x}_1, \bar{M}_1} \circ \Phi_{x', M'} \circ \Phi_{\bar{x}_2, \bar{M}_2} \right\}, \quad (27)$$

which fulfils the condition

$$\mathcal{K}(\Phi_{x', M'}) \geq \mathcal{K}(\Phi_{x, M}), \quad \forall (x', M') \in \mathbb{H}_{x, M}. \quad (28)$$

Notice that by construction $\mathbb{L}_{x,M}$ and $\mathbb{H}_{x,M}$ obey a natural ordering

$$\mathbb{L}_{x', M'} \subseteq \mathbb{L}_{x, M} \quad \forall (x', M') \in \mathbb{L}_{x, M}, \quad (29)$$

$$\mathbb{H}_{x', M'} \subseteq \mathbb{H}_{x, M} \quad \forall (x', M') \in \mathbb{H}_{x, M}, \quad (30)$$

and fulfil the complementary relation

$$(x', M') \in \mathbb{H}_{x, M} \iff (x, M) \in \mathbb{L}_{x', M'}. \quad (31)$$

In the next subsections we shall provide an analytic characterization of $\mathbb{L}_{x,M}$ and $\mathbb{H}_{x,M}$. As we shall see one can identify two different regimes ruled by the function $M_{\text{EB}}(x)$ of Eq. (10) which identifies the EB sector. Indeed for points (x, M) with

$$M \leq M_{\text{EB}}(x) = \min\{1, x\}, \quad (32)$$

that is for channels which are non-EB and for the EB ones which are on the border line of the region \mathbb{EB} , the sets $\mathbb{L}_{x,M}$ and $\mathbb{H}_{x,M}$ are defined by the functions

$$f_{x,M}^{(1)}(x') := M + (1-x)\Theta(1-x) + (x'-1)\Theta(1-x'), \\ f_{x,M}^{(2)}(x') := (x'/x)[M + (x-1)\Theta(x-1)] \\ - (x'-1)\Theta(x'-1), \quad (33)$$

with $\Theta(x)$ being the Heaviside step-function. Specifically we shall prove that under the condition (32), $\mathbb{L}_{x,M}$ is formed by all points which are above $f_{x,M}^{(1)}(x')$ and $f_{x,M}^{(2)}(x')$, i.e.

$$\mathbb{L}_{x,M} = \left\{ (x', M') \in (\mathbb{R}^+)^2 : \right. \\ \left. M' \geq \max\{f_{x,M}^{(1)}(x'), f_{x,M}^{(2)}(x')\} \right\}, \quad (34)$$

while $\mathbb{H}_{x,M}$ is given by the polytope formed by the points below such curves, i.e.

$$\mathbb{H}_{x,M} = \left\{ (x', M') \in (\mathbb{R}^+)^2 : \right. \\ \left. M' \leq \min\{f_{x,M}^{(1)}(x'), f_{x,M}^{(2)}(x')\} \right\}. \quad (35)$$

As evident from Fig. 3, the domains identified by Eqs. (34) and (35) admit (x, M) as unique contact point, implying that for a relative large portion of the phase space $(\mathbb{R}^+)^2$ we cannot assign a definite ordering w.r.t. $\mathcal{K}(\Phi_{x,M})$ (white regions of plots). The situation change however when the map $\Phi_{x,M}$ is deep inside the EB region, i.e. for

$$M > M_{\text{EB}}(x) = \min\{1, x\}. \quad (36)$$

Under the constraint (36) the sets $\mathbb{H}_{x,M}$ and $\mathbb{L}_{x,M}$ provide a complete covering of the phase space and have a non trivial overlap $\mathbb{O}_{x,M} := \mathbb{H}_{x,M} \cap \mathbb{L}_{x,M}$. Indeed, one can show that irrespectively from the specific choice of (x, M) , $\mathbb{H}_{x,M}$ coincides with the entire space $(\mathbb{R}^+)^2$, i.e.

$$\mathbb{H}_{x,M} = (\mathbb{R}^+)^2, \quad (37)$$

while $\mathbb{L}_{x,M}$ (and hence $\mathbb{O}_{x,M}$) corresponds to the $x \rightarrow 0, M \rightarrow 0$, limit of Eq. (34), i.e. [55]

$$\mathbb{L}_{x,M} = \mathbb{O}_{x,M} \\ = \mathbb{L}_{0,0} := \left\{ (x', M') \in (\mathbb{R}^+)^2 : M' > M_{\text{EB}}(x') \right\}, \quad (38)$$

which coincides with the subset identified by Eq. (36). This implies that given any two points (x_1, M_1) and (x_2, M_2) in $\mathbb{L}_{0,0}$, their associated channel are equivalent up to concatenation with extra GBCs (3), i.e. there exist proper choices of the maps $\Phi_{\bar{x}_1, \bar{M}_1}, \Phi_{\bar{x}_2, \bar{M}_2}, \Phi_{\bar{x}_3, \bar{M}_3}$, and $\Phi_{\bar{x}_4, \bar{M}_4}$, such that we can write

$$\begin{cases} \Phi_{x_1, M_1} = \Phi_{\bar{x}_1, \bar{M}_1} \circ \Phi_{x_2, M_2} \circ \Phi_{\bar{x}_2, \bar{M}_2}, \\ \Phi_{x_2, M_2} = \Phi_{\bar{x}_3, \bar{M}_3} \circ \Phi_{x_1, M_1} \circ \Phi_{\bar{x}_4, \bar{M}_4}, \end{cases} \quad (39)$$

which in turn imposes $\mathcal{K}(\Phi_{x_1, M_1}) = \mathcal{K}(\Phi_{x_2, M_2})$ in agreement with the property (11).

V. ANALYTICAL CHARACTERIZATION OF $\mathbb{L}_{x,M}$ AND $\mathbb{H}_{x,M}$

In this section we give an analytical characterization of the low-ground and high-ground regions for an arbitrary channel $\Phi_{x,M}$. We start in Sec. V A by focusing on a simplified version of the concatenation rules entering in the definitions (24) and (27) where $\Phi_{x,M}$ is connected with the elements $\Phi_{x', M'}$ via only a single extra PI-GBC element $\Phi_{\bar{x}, \bar{M}}$. This will allows us to identify two regions

$$\mathbb{L}_{x,M}^{(0)} := \left\{ (x', M') \in (\mathbb{R}^+)^2 : \exists (\bar{x}, \bar{M}) \in (\mathbb{R}^+)^2 \right. \\ \left. \Phi_{x', M'} = \Phi_{\bar{x}, \bar{M}} \circ \Phi_{x, M} \text{ or } \Phi_{x', M'} = \Phi_{x, M} \circ \Phi_{\bar{x}, \bar{M}} \right\}, \quad (40)$$

and

$$\mathbb{H}_{x,M}^{(0)} := \left\{ (x', M') \in (\mathbb{R}^+)^2 : \exists (\bar{x}, \bar{M}) \in (\mathbb{R}^+)^2 \right. \\ \left. \Phi_{x, M} = \Phi_{\bar{x}, \bar{M}} \circ \Phi_{x', M'} \text{ or } \Phi_{x, M} = \Phi_{x', M'} \circ \Phi_{\bar{x}, \bar{M}} \right\}. \quad (41)$$

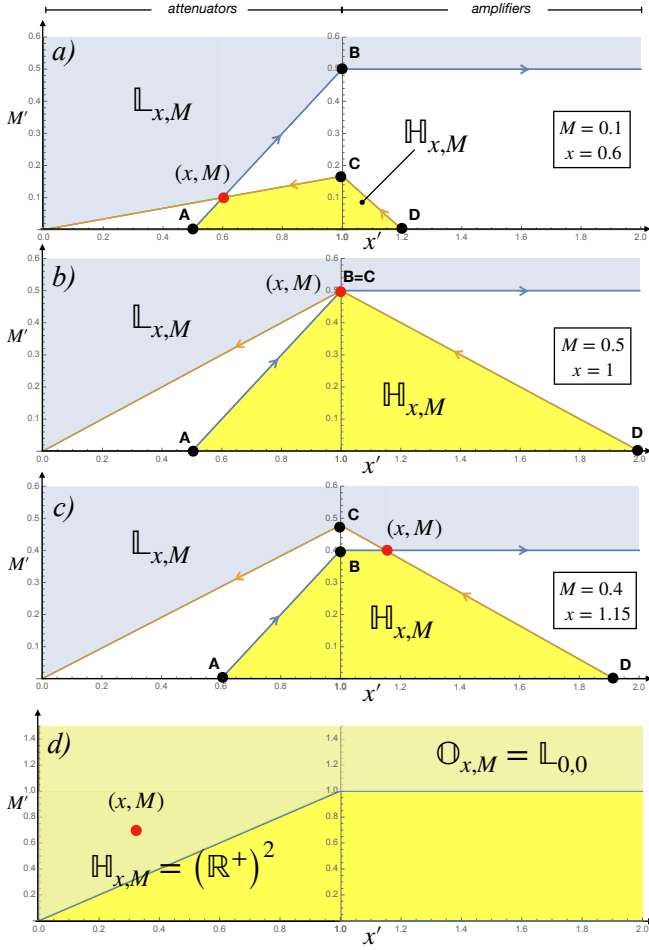


FIG. 3: Low-ground capacity region $\mathbb{L}_{x,M}$ (24) (light blue area) and high-ground capacity region $\mathbb{H}_{x,M}$ (27) (yellow) for the channel $\Phi_{x,M}$ (red dot element). The first three top panels refer to the regime (32) where $\mathbb{L}_{x,M}$ and $\mathbb{H}_{x,M}$ are expressed respectively by Eqs. (34) and (35): specifically in panel a) the reference map is an attenuator ($x = 0.6$, $M = 0.1$), in panel b) it is an additive classical noise map ($x = 1$, $M = 0.5$), and in panel c) it is an amplifier ($x = 1.15$, $M = 0.1$). Panel d) instead presents a case where $\Phi_{x,M}$ fulfils the EB condition (36); here $\mathbb{H}_{x,M}$ coincides with the full plane $(\mathbb{R}^+)^2$, while $\mathbb{L}_{x,M}$ (and hence the overlap $\mathbb{O}_{x,M} = \mathbb{H}_{x,M} \cap \mathbb{L}_{x,M}$), are given by the set $\mathbb{L}_{0,0}$ of Eq. (38): by construction any two points in this area are equivalent under GBC concatenation, see Eq. (39). The border lines which identify the various regions are the functions $f_{x,M}^{(1)}(x')$ (blue curve) and $f_{x,M}^{(2)}(x')$ (orange curve) defined in Eq. (33) – for panel d) the border is given by $f_{0,0}^{(1)}(x') = \min\{1, x'\}$ [55]. The arrows in the plots show the direction where the capacities have to decrease (or at most remain constant) and the white regions describe portions of the parameter space where the composition rules cannot be used to determine a specific capacity ordering with respect to the reference channel. In panel a) we have $\mathbf{A} = (x - M, 0)$, $\mathbf{B} = (1, M - x + 1)$, $\mathbf{C} = (1, M/x)$, $\mathbf{D} = (x/(x - M), 0)$; in panel b) and c) instead $\mathbf{A} = (1 - M, 0)$, $\mathbf{B} = (1, M)$, $\mathbf{C} = (1, (M + x - 1)/x)$, $\mathbf{D} = (x/(1 - M), 0)$ (notice that for b), $\mathbf{B} = \mathbf{C} = (x, M)$).

which by construction are subsets of $\mathbb{L}_{x,M}$ and $\mathbb{H}_{x,M}$, i.e.

$$\mathbb{L}_{x,M}^{(0)} \subseteq \mathbb{L}_{x,M}, \quad \mathbb{H}_{x,M}^{(0)} \subseteq \mathbb{H}_{x,M}. \quad (42)$$

In Sec. VB we shall prove that for (x, M) fulfilling the constraint (32), $\mathbb{L}_{x,M}^{(0)}$ and $\mathbb{H}_{x,M}^{(0)}$ indeed coincide with $\mathbb{L}_{x,M}$ and $\mathbb{H}_{x,M}$ leading to Eqs. (34) and (35). The derivation of Eqs. (37) and (38) for maps not fulfilling (32) will instead be given in Sec. VC.

A. Two-elements concatenations

To determine $\mathbb{L}_{x,M}^{(0)}$ and $\mathbb{H}_{x,M}^{(0)}$ we adopt the parametrization (4) to better underline the role played by amplifiers and attenuators. Given hence $\eta \in [0, 1]$ and $N \geq 0$, let us introduce the following functions

$$N_{\eta,N}^{(1)}(\eta') := N \left(\frac{1-\eta}{1-\eta'} \right) \left(\frac{\eta'}{1-\eta'} \right), \quad (43)$$

$$N_{\eta,N}^{(2)}(\eta') := (N + 1) \left(\frac{1-\eta}{1-\eta'} \right) - 1. \quad (44)$$

It then turns out that

Property 1. *The attenuator map $\mathcal{E}_{\eta,N}$ admits*

$$\begin{cases} \mathbb{L}_{\eta,N}^{(\text{att},1)} &:= \{(\eta', N') : 0 \leq \eta' \leq \eta, N' \geq \max\{N_{\eta,N}^{(1)}(\eta'), 0\}\}, \\ \mathbb{L}_{\eta,N}^{(\text{att},2)} &:= \{(\eta', N') : 1 \geq \eta' \geq \eta, N' \geq \max\{N_{\eta,N}^{(2)}(\eta'), 0\}\}, \\ \mathbb{L}_{\eta,N}^{(\text{att})} &:= \mathbb{L}_{\eta,N}^{(\text{att},1)} \cup \mathbb{L}_{\eta,N}^{(\text{att},2)}, \end{cases} \quad (45)$$

(light blue area on the left-hand-side of the top panel of Fig. 4), as subset of the corresponding two-element concatenation, low-ground capacity region $\mathbb{L}^{(0)}(\mathcal{E}_{\eta,N})$, and

$$\begin{cases} \mathbb{H}_{\eta,N}^{(\text{att},1)} &:= \{(\eta', N') : 1 \geq \eta' \geq \eta, 0 \leq N' \leq N_{\eta,N}^{(1)}(\eta')\}, \\ \mathbb{H}_{\eta,N}^{(\text{att},2)} &:= \{(\eta', N') : 1 \leq \eta' \leq \eta, 0 \leq N' \leq N_{\eta,N}^{(2)}(\eta')\}, \\ \mathbb{H}_{\eta,N}^{(\text{att})} &:= \mathbb{H}_{\eta,N}^{(\text{att},1)} \cup \mathbb{H}_{\eta,N}^{(\text{att},2)}, \end{cases} \quad (46)$$

(yellow area on the left-hand-side of top panel of Fig. 4) as subset of $\mathbb{H}^{(0)}(\mathcal{E}_{\eta,N})$, i.e.

$$\mathbb{L}_{\eta,N}^{(\text{att})} \subseteq \mathbb{L}^{(0)}(\mathcal{E}_{\eta,N}), \quad \mathbb{H}_{\eta,N}^{(\text{att})} \subseteq \mathbb{H}^{(0)}(\mathcal{E}_{\eta,N}). \quad (47)$$

Proof. To derive the first inclusion of Eq. (47) we set $(\eta_3, N_3) = (\eta', N')$ and $(\eta_1, N_1) = (\eta, N)$ in Eq. (C₁) of Tab. I to observe that for all $\eta_2 \in [0, 1]$ and $N_2 \geq 0$,

$$\mathcal{E}_{\eta',N'} = \mathcal{E}_{\eta_2,N_2} \circ \mathcal{E}_{\eta,N}, \quad (48)$$

is also a thermal channel with parameters

$$\begin{cases} \eta' = \eta \eta_2 \leq \eta, \\ N' = \frac{(1-\eta)\eta_2 N + (1-\eta_2)N_2}{1-\eta\eta_2} \geq \frac{(1-\eta)\eta_2}{1-\eta\eta_2} N = N_{\eta,N}^{(1)}(\eta'), \end{cases} \quad (49)$$

that span the entire set $\mathbb{L}_{\eta,N}^{(\text{att},1)}$, as the inequality is saturated whenever $N_2 = 0$. Therefore in view of the definition (24) we can conclude that

$$\mathbb{L}_{\eta,N}^{(\text{att},1)} \subseteq \mathbb{L}^{(0)}(\mathcal{E}_{\eta,N}). \quad (50)$$

We next invoke Eq. (C_{3.1}) of Tab. I to observe that

$$\mathcal{E}_{\eta',N'} = \mathcal{E}_{\eta,N} \circ \mathcal{A}_{g_1,N_1}, \quad (51)$$

with

$$\begin{cases} \eta' = g_1 \eta \geq \eta, \\ N' = \frac{(1-\eta)(2N+1) + \eta(g_1-1)(2N_1+1) - (1-\eta')}{2(1-\eta')} \\ \geq \frac{\eta' - \eta + (1-\eta)N}{1-\eta'} = N_{\eta,N}^{(2)}(\eta'), \end{cases} \quad (52)$$

is a thermal map too which spans the entire subset $\mathbb{L}_{\eta,N}^{(\text{att},2)}$, as the inequality is saturated whenever $N_1 = 0$. Accordingly we can claim that

$$\mathbb{L}_{\eta,N}^{(\text{att},2)} \subseteq \mathbb{L}^{(0)}(\mathcal{E}_{\eta,N}), \quad (53)$$

which together with (50) yields the first identity of Eq. (47). The derivation of the second identity of Eq. (47) follows along the same lines by simply inverting the roles of (η', N') and (η, N) in the previous passages. \square

Given next $g \geq 1$ and $N \geq 0$ and the functions

$$N_{g,N}^{(1)}(g') := N \left(\frac{g-1}{g'-1} \right), \quad (54)$$

$$N_{g,N}^{(2)}(g') := (N+1) \left(\frac{g-1}{g'} \right) \left(\frac{g'}{g'-1} \right) - 1. \quad (55)$$

We can show that

Property 2. *The amplifier channel $\mathcal{A}_{g,N}$ admits*

$$\begin{cases} \mathbb{L}_{g,N}^{(\text{amp},1)} &:= \{(g', N') : g' \geq g, N' \geq \max\{N_{g,N}^{(1)}(g'), 0\}\}, \\ \mathbb{L}_{g,N}^{(\text{amp},2)} &:= \{(g', N') : g' \leq g, N' \geq \max\{N_{g,N}^{(2)}(g'), 0\}\}, \\ \mathbb{L}_{g,N}^{(\text{amp})} &:= \mathbb{L}_{g,N}^{(\text{amp},1)} \cup \mathbb{L}_{g,N}^{(\text{amp},2)}, \end{cases} \quad (56)$$

(light blue area on the right-hand-side of the bottom panel of Fig. 4), as subset of the corresponding two-element concatenation, low-ground capacity region $\mathbb{L}^{(0)}(\mathcal{A}_{\eta,N})$, and

$$\begin{cases} \mathbb{H}_{g,N}^{(\text{amp},1)} &:= \{(g', N') : 1 \leq g' \leq g, 0 \leq N' \leq N_{g,N}^{(1)}(g')\}, \\ \mathbb{H}_{g,N}^{(\text{amp},2)} &:= \{(g', N') : g' \geq g, 0 \leq N' \leq N_{g,N}^{(2)}(g')\}, \\ \mathbb{H}_{g,N}^{(\text{amp})} &:= \mathbb{H}_{g,N}^{(\text{amp},1)} \cup \mathbb{H}_{g,N}^{(\text{amp},2)}, \end{cases} \quad (57)$$

(yellow area on the right-hand-side of bottom panel of Fig. 4), as subspace of $\mathbb{H}^{(0)}(\mathcal{A}_{\eta,N})$, i.e.

$$\mathbb{L}_{g,N}^{(\text{amp})} \subseteq \mathbb{L}^{(0)}(\mathcal{A}_{g,N}), \quad \mathbb{H}_{g,N}^{(\text{amp})} \subseteq \mathbb{H}^{(0)}(\mathcal{A}_{g,N}). \quad (58)$$

Proof. To derive the first inclusion we set $(g_3, N_3) = (g', N')$ and $(g_2, N_2) = (g, N)$ in Eq. (C₂) of Tab. I to observe for all $g_1 \geq 1$ and $N_1 \geq 0$,

$$\mathcal{A}_{g',N'} = \mathcal{A}_{g,N} \circ \mathcal{A}_{g_1,N_1} \quad (59)$$

is also a thermal channel with parameters

$$\begin{cases} g' = g_1 g \geq g, \\ N' = \frac{(g_1-1)gN_1 + (g-1)N}{g'-1} \geq N_{g,N}^{(1)}(g'), \end{cases} \quad (60)$$

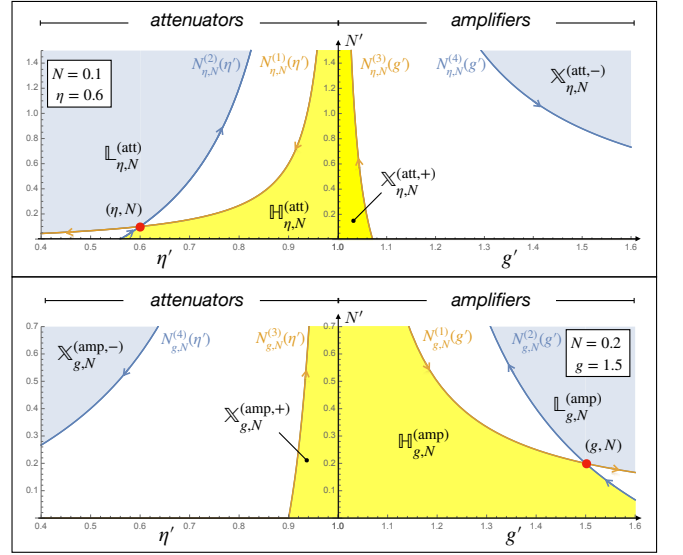


FIG. 4: Two-element concatenation analysis of the low-ground and high-ground capacity regions for thermal attenuators and amplifiers (for all the examples reported in the plots the channels are non-EB, i.e. fulfil the condition (32)). Top panel: given a thermal attenuator $\mathcal{E}_{\eta,N}$ (red dot element), the light blue areas correspond respectively to $\mathbb{L}_{\eta,N}^{(\text{att})}$ and $\mathbb{X}_{\eta,N}^{(\text{att},-)}$; the yellow areas describe instead $\mathbb{H}_{\eta,N}^{(\text{att})}$ and $\mathbb{X}_{\eta,N}^{(\text{att},+)}$. Plot realized using $N = 0.1$ and $\eta = 0.6$. Bottom panel: given a thermal amplifier $\mathcal{A}_{g,N}$ (red dot element), the light blue area describe the sets $\mathbb{L}_{g,N}^{(\text{amp})}$ and $\mathbb{X}_{g,N}^{(\text{amp},-)}$ while the yellow area $\mathbb{H}_{g,N}^{(\text{amp})}$ and $\mathbb{X}_{g,N}^{(\text{amp},+)}$. Plot realized using $N = 0.2$ and $g = 1.5$. The orange and blue curves represent the border lines of the low ground/high ground regions defined by the functions $N_{\eta,N}^{(1,2)}(\eta')$ of Eqs. (43), (44), $N_{\eta,N}^{(3,4)}(g')$ of Eqs. (65), (66), $N_{g,N}^{(1,2)}(g')$ of Eqs. (54), (55), and $N_{g,N}^{(3,4)}(g')$ of Eqs. (71), (72): along these curves the arrows show the direction where the capacities have to decrease (or at most remain constant) – see Corollaries 4.2 and 4.3 of App. A. For the points in the white regions the composition rules cannot be used to determine a specific capacity ordering with respect to the capacity of the red dot element.

which span the entire area $\mathbb{L}_{g,N}^{(\text{amp},1)}$, as the inequality is saturated whenever $N_1 = 0$, leading to

$$\mathbb{L}_{g,N}^{(\text{amp},1)} \subseteq \mathbb{L}^{(0)}(\mathcal{A}_{g,N}). \quad (61)$$

We next invoke (C_{3.2}) of Tab. I to observe that

$$\mathcal{A}_{g',N'} = \mathcal{E}_{\eta_2,N_2} \circ \mathcal{A}_{g,N}, \quad (62)$$

is an amplifier too with parameters

$$\begin{cases} g' = \eta_2 g \leq g, \\ N' = \frac{(1-\eta_2)(2N_2+1) + \eta_2(g-1)(2N+1) - (g'-1)}{2(g'-1)} \geq N_{g,N}^{(2)}(g'), \end{cases} \quad (63)$$

that cover the entire subset $\mathbb{L}_{g,N}^{(\text{amp},2)}$, as the inequality is

saturated whenever $N_2 = 0$. Hence we have

$$\mathbb{L}_{g,N}^{(\text{amp},1)} \subseteq \mathbb{L}^{(0)}(\mathcal{A}_{g,N}) . \quad (64)$$

which together with (64) gives us the thesis. The derivation of the second inclusion of Eq. (68) follows along the same lines by simply inverting the roles of (g', N') and (g, N) in the previous passages. \square

It is finally possible to establish a partial ordering between the capacities of attenuators and those of the amplifiers. Specifically given $\eta \in [0, 1]$ and $N \geq 0$ and the functions

$$N_{\eta,N}^{(3)}(g) := N \left(\frac{1-\eta}{\eta} \right) \left(\frac{g}{g-1} \right) - 1 , \quad (65)$$

$$N_{\eta,N}^{(4)}(g) := (N+1) \left(\frac{1-\eta}{g-1} \right) , \quad (66)$$

it follows that

Property 3. *The attenuator map $\mathcal{E}_{\eta,N}$ admits*

$$\mathbb{X}_{\eta,N}^{(\text{att},+)} := \left\{ (g, N') : g \geq 1, 0 \leq N' \leq N_{\eta,N}^{(3)}(g) \right\} , \quad (67)$$

$$\mathbb{X}_{\eta,N}^{(\text{att},-)} := \left\{ (g, N') : g \geq 1, N' \geq \max\{N_{\eta,N}^{(4)}(g), 0\} \right\} ,$$

(yellow and light blue areas on the right-hand-side of the top panel of Fig. 4) as subsets of $\mathbb{H}^{(0)}(\mathcal{E}_{\eta,N})$ and $\mathbb{L}^{(0)}(\mathcal{E}_{\eta,N})$ respectively, i.e.

$$\mathbb{X}_{\eta,N}^{(\text{att},+)} \subseteq \mathbb{H}^{(0)}(\mathcal{E}_{\eta,N}) , \quad \mathbb{X}_{\eta,N}^{(\text{att},-)} \subseteq \mathbb{L}^{(0)}(\mathcal{E}_{\eta,N}) . \quad (68)$$

Proof. To prove the first inclusion we use the decomposition rule (**C3.1**) of Tab. I, which setting $(\eta_3, N_3) = (\eta, N)$, $(g_1, N_1) = (g, N')$, and arbitrary $\eta_2 \in [0, 1]$, $N_2 \geq 0$, allows us to write

$$\mathcal{E}_{\eta,N} = \mathcal{E}_{\eta_2,N_2} \circ \mathcal{A}_{g,N'} , \quad (69)$$

for all $g \geq 1$ and $N' \leq N_{\eta,N}^{(3)}(g)$, i.e. for the entire set $\mathbb{X}_{\eta,N}^{(\text{att},+)}$. The second inclusion follows instead from Eq. (**C3.2**) of Tab. I, which setting $(\eta_2, N_2) = (\eta, N)$, $(g_3, N_3) = (g, N')$, and arbitrary $g_1 \geq 1$, $N_1 \geq 0$ allows us to write

$$\mathcal{A}_{g,N'} = \mathcal{E}_{\eta,N} \circ \mathcal{A}_{g_1,N_1} , \quad (70)$$

for all $g \geq 1$ and $N' \geq N_{\eta,N}^{(4)}(g)$, i.e. for the entire set $\mathbb{X}_{\eta,N}^{(\text{att},-)}$. \square

In a similar way, given

$$N_{g,N}^{(3)}(\eta) := N \left(\frac{g-1}{1-\eta} \right) - 1 , \quad (71)$$

$$N_{g,N}^{(4)}(\eta) := (N+1) \left(\frac{g-1}{g} \right) \left(\frac{\eta}{1-\eta} \right) , \quad (72)$$

we have that

Property 4. *The amplifier map $\mathcal{A}_{g,N}$ admits*

$$\mathbb{X}_{g,N}^{(\text{amp},+)} := \left\{ (\eta, N') : \eta \in [0, 1], 0 \leq N' \leq N_{g,N}^{(3)}(\eta) \right\} , \quad (73)$$

$$\mathbb{X}_{g,N}^{(\text{amp},-)} := \left\{ (\eta, N') : g \geq 1, N' \geq \max\{N_{g,N}^{(4)}(\eta), 0\} \right\} ,$$

(yellow and light blue areas on the left-hand-side of the bottom panel of Fig. 4) as subsets of $\mathbb{H}^{(0)}(\mathcal{A}_{g,N})$ and $\mathbb{L}^{(0)}(\mathcal{A}_{g,N})$ respectively, i.e.

$$\mathbb{X}_{g,N}^{(\text{amp},+)} \subseteq \mathbb{H}^{(0)}(\mathcal{A}_{g,N}) , \quad \mathbb{X}_{g,N}^{(\text{amp},-)} \subseteq \mathbb{L}^{(0)}(\mathcal{A}_{g,N}) . \quad (74)$$

Proof. The above inclusions are just an alternative way to cast the results of Property 3. For the sake of symmetry we provide however an independent derivation. The first can be proven by using the decomposition rule (**C3.2**) of Tab. I, which setting $(g_3, N_3) = (g, N)$, $(\eta_2, N_2) = (\eta, N')$, and $g_1 \geq 1$, $N_1 \geq 0$, allows us to write

$$\mathcal{A}_{g,N} = \mathcal{E}_{\eta,N'} \circ \mathcal{A}_{g_1,N_1} , \quad (75)$$

for all $\eta \in [0, 1]$ and $0 \leq N' \leq N_{g,N}^{(3)}(\eta)$, i.e. for all the points of $\mathbb{X}_{g,N}^{(\text{amp},+)}$. The second inclusion of Eq. (74) follows instead from Eq. (**C3.1**) of Tab. I, which setting $(\eta_3, N_3) = (\eta, N')$, $(g_1, N_1) = (g, N)$, and $\eta_2 \in [0, 1]$, $N_2 \geq 0$, gives us

$$\mathcal{E}_{\eta,N'} = \mathcal{E}_{\eta_2,N_2} \circ \mathcal{A}_{g,N} , \quad (76)$$

for all $\eta \in [0, 1]$ and $N' \geq N_{g,N}^{(4)}(\eta)$, i.e. for all the points of $\mathbb{X}_{g,N}^{(\text{amp},-)}$. \square

Inclusions which are different with respect to the one reported in the Properties can be obtained by reversing the order of the decompositions employed in the proofs. Such inequalities however are provably less performant than those presented. For instance setting $(\eta_3, N_3) = (\eta', N')$ and $(\eta_2, N_2) = (\eta, N)$ in Eq. (**C1**) allows us to determine that $(\eta', N') \in \mathbb{L}(\mathcal{E}_{\eta,N})$ for all

$$\eta' \leq \eta , \quad N' \geq \left(\frac{1-\eta}{1-\eta'} \right) N , \quad (77)$$

a result which is implied by (50) since the set $\mathbb{L}_{\eta,N}^{(\text{att},2)}$ includes all points fulfilling the condition (77). Similarly using Eq. (**C4.1**) instead of (**C3.1**) allows one to show that i) $(\eta', N') \in \mathbb{L}(\mathcal{E}_{\eta,N})$ for all $\eta' \geq \eta$ and $N' \geq \frac{\eta'-\eta+\eta'(1-\eta)N}{\eta(1-\eta')}$ (a condition that is already implied by (47)); ii) $(\eta', N') \in \mathbb{H}(\mathcal{E}_{\eta,N})$ for all $\eta' \leq \eta$ and $N' \leq \frac{\eta'-\eta+\eta'(1-\eta)N}{\eta(1-\eta')}$ (which again is implied by (47)); iii) $(g, N') \in \mathbb{H}(\mathcal{E}_{\eta,N})$ for all $g \geq 1$ and $N' \leq N \left(\frac{1-\eta}{g-1} \right) - 1$ (implied by the first inclusion of Eq. (68)); iv) $(g, N') \in \mathbb{L}(\mathcal{E}_{\eta,N})$ for all $g \geq 1$ and $N' \geq (N+1) \left(\frac{g-1}{g} \right) \left(\frac{1-\eta}{1-\eta} \right)$ (implied by the second inclusion of Eq. (68)). Putting together these results we can hence conclude that the two-elements concatenation

regions $\mathbb{L}^{(0)}(\mathcal{E}_{\eta,N})$ and $\mathbb{L}^{(0)}(\mathcal{A}_{g,N})$ coincide respectively with $\mathbb{L}_{\eta,N}^{(\text{att})} \cup \mathbb{X}_{\eta,N}^{(\text{att},-)}$ and $\mathbb{L}_{g,N}^{(\text{amp})} \cup \mathbb{X}_{g,N}^{(\text{amp},-)}$, a condition which translated into the parametrization (3) can be expressed as

$$\mathbb{L}_{x,M}^{(0)} = \begin{cases} \mathbb{L}_{x,M/(1-x)}^{(\text{att})} \cup \mathbb{X}_{x,M/(1-x)}^{(\text{att},-)} & \text{for } x \in [0, 1], \\ \mathbb{L}_{x,M/(x-1)}^{(\text{amp})} \cup \mathbb{X}_{x,M/(x-1)}^{(\text{amp},-)} & \text{for } x \geq 1. \end{cases} \quad (78)$$

Analogously we have that $\mathbb{H}^{(0)}(\mathcal{E}_{\eta,N})$ and $\mathbb{H}^{(0)}(\mathcal{A}_{g,N})$ correspond respectively to $\mathbb{H}_{\eta,N}^{(\text{att})} \cup \mathbb{X}_{\eta,N}^{(\text{att},+)}$ and $\mathbb{H}_{g,N}^{(\text{amp})} \cup \mathbb{X}_{g,N}^{(\text{amp},+)}$, so that

$$\mathbb{H}_{x,M}^{(0)} = \begin{cases} \mathbb{H}_{x,M/(1-x)}^{(\text{att})} \cup \mathbb{X}_{x,M/(1-x)}^{(\text{att},+)} & \text{for } x \in [0, 1], \\ \mathbb{H}_{x,M/(x-1)}^{(\text{amp})} \cup \mathbb{X}_{x,M/(x-1)}^{(\text{amp},+)} & \text{for } x \geq 1. \end{cases} \quad (79)$$

The border lines of these regions are provided by the curves $M_{x,M}^{(j)}(x')$ of Tab. II obtained from $N_{\eta,N}^{(1,2)}(\eta')$, $N_{g,N}^{(1,2)}(g')$, $N_{\eta,N}^{(3,4)}(g')$, and $N_{g,N}^{(1,2)}(\eta')$ via the substitutions

$$M_{x,M}^{(j)}(x') := |1 - x'| N_{x,M/|1-x|}^{(j)}(x'). \quad (80)$$

For instance one has that $\mathbb{L}_{x,M}^{(0)}$ is given by the points (x', M') such that

$$M' \geq \begin{cases} M_{x,M}^{(1)}(x') = M \frac{x'}{x}, & (0 \leq x' \leq x), \\ M_{x,M}^{(2)}(x') = M - x + x', & (x \leq x' \leq 1), \\ M_{x,M}^{(4)}(x') = M + 1 - x, & (1 \leq x'), \end{cases} \quad (81)$$

for $x \leq 1$, and

$$M' \geq \begin{cases} M_{x,M}^{(4)}(x') = (M + x - 1) \frac{x'}{x}, & (0 \leq x' \leq 1), \\ M_{x,M}^{(2)}(x') = (M - 1) \frac{x'}{x} + 1, & (1 \leq x' \leq x), \\ M_{x,M}^{(1)}(x') = M, & (x \leq x'), \end{cases} \quad (82)$$

for $x \geq 1$. Viceversa we have that $\mathbb{H}_{x,M}^{(0)}$ includes all points (x', M') such that

$$0 \leq M' \leq \begin{cases} M_{x,M}^{(2)}(x') = M - x + x', & (0 \leq x' \leq x), \\ M_{x,M}^{(1)}(x') = M \frac{x'}{x}, & (x \leq x' \leq 1), \\ M_{x,M}^{(3)}(x') = (M - x) \frac{x'}{x} + 1, & (1 \leq x'), \end{cases} \quad (83)$$

for $x \leq 1$, and

$$0 \leq M' \leq \begin{cases} M_{x,M}^{(3)}(x') = M - 1 + x', & (0 \leq x' \leq 1), \\ M_{x,M}^{(1)}(x') = M, & (1 \leq x' \leq x), \\ M_{x,M}^{(2)}(x') = (M - 1) \frac{x'}{x} + 1, & (x \leq x'), \end{cases} \quad (84)$$

for $x \geq 1$.

B. Three-elements concatenation regions for channels $\Phi_{x,M}$ fulfilling Eq. (32)

Comparing the l.h.s. of Eqs. (81)–(84) with the functions $f_{x,M}^{(1)}(x')$ and $f_{x,M}^{(2)}(x')$ of Eq. (33), one can easily check that for channels $\Phi_{x,M}$ which fulfil Eq. (32), the two-element concatenation regions $\mathbb{L}_{x,M}^{(0)}$ and $\mathbb{H}_{x,M}^{(0)}$ can be expressed as

$$\mathbb{L}_{x,M}^{(0)} = \left\{ (x', M') \in (\mathbb{R}^+)^2 : \right. \\ \left. M' \geq \max\{f_{x,M}^{(1)}(x'), f_{x,M}^{(2)}(x')\} \right\}, \quad (85)$$

$$\mathbb{H}_{x,M}^{(0)} = \left\{ (x', M') \in (\mathbb{R}^+)^2 : \right. \\ \left. M' \leq \min\{f_{x,M}^{(1)}(x'), f_{x,M}^{(2)}(x')\} \right\}. \quad (86)$$

Accordingly under the condition (32), the proof of the identities (34) and (35) reduces hence to show that the two-element concatenation regions $\mathbb{L}_{x,M}^{(0)}$ and $\mathbb{H}_{x,M}^{(0)}$ correspond to the three-elements concatenations sets $\mathbb{L}_{x,M}$ and $\mathbb{H}_{x,M}$, i.e.

Corollary 4.1. *Given (x, M) such that $M \leq M_{EB}(x)$ we have that*

$$\mathbb{L}_{x,M}^{(0)} = \mathbb{L}_{x,M}, \quad \mathbb{H}_{x,M}^{(0)} = \mathbb{H}_{x,M}. \quad (87)$$

Proof. This result can be derived by noticing that for channels $\Phi_{x,M}$ which are non-EB, $\mathbb{L}_{x,M}^{(0)}$ and $\mathbb{H}_{x,M}^{(0)}$ fulfil the same ordering rules of $\mathbb{L}_{x,M}$ and $\mathbb{H}_{x,M}$ given in Eqs. (29) and (30), i.e.

$$M < M_{EB}(x) \implies \begin{cases} \mathbb{L}_{x',M'}^{(0)} \subseteq \mathbb{L}_{x,M}^{(0)}, \forall (x', M') \in \mathbb{L}_{x,M}^{(0)} \\ \mathbb{H}_{x',M'}^{(0)} \subseteq \mathbb{H}_{x,M}^{(0)}, \forall (x', M') \in \mathbb{H}_{x,M}^{(0)} \end{cases} \quad (88)$$

The derivation of these identities relies on a series geometric relations in which one has to compare the relative size and position of the two-dimensional polytopes defined in Eqs. (93) and (94). It suffices to do show this for the high ground region. In fact, since $(x', M') \in \mathbb{L}_{x,M}^{(0)}$ if and only if $(x, M) \in \mathbb{H}_{x',M'}^{(0)}$, we have that $(x'', M'') \in \mathbb{L}_{x,M}^{(0)}$, $(x'', M'') \in \mathbb{L}_{x',M'}^{(0)}$, $(x', M') \in \mathbb{L}_{x,M}^{(0)}$ if and only if $(x, M) \in \mathbb{H}_{x'',M''}^{(0)}$, $(x', M') \in \mathbb{H}_{x'',M''}^{(0)}$, $(x, M) \in \mathbb{H}_{x',M'}^{(0)}$. Therefore it suffices to prove only that the latter is true whenever $(x', M') \in \mathbb{H}_{x'',M''}^{(0)}$ and $(x, M) \in \mathbb{H}_{x',M'}^{(0)}$. This can be proven by case-by-case inspection, and we outline the derivation with the aid of Fig. 5. Take hence $(x', M') \in \mathbb{L}_{x,M}$: from (24) it follows that we can write

$$\Phi_{x',M'} = \Phi_{\bar{x}_1, \bar{M}_1} \circ \Phi_{x,M} \circ \Phi_{\bar{x}_2, \bar{M}_2}, \quad (89)$$

for some proper choice of $(\bar{x}_1, \bar{M}_1), (\bar{x}_2, \bar{M}_2) \in (\mathbb{R}^+)^2$. Setting then $\Phi_{x_2, M_2} := \Phi_{x,M} \circ \Phi_{\bar{x}_2, \bar{M}_2}$, we can claim that (x_2, M_2) is an element of $\mathbb{L}_{x,M}^{(0)}$ and (x', M') an element

$N_{\eta,N}^{(1)}(\eta') \mapsto M_{x,M}^{(1)}(x') := (1 - \eta')N_{\eta,N}^{(1)}(\eta')$	$\left \begin{array}{l} \eta=x, \eta'=x' \\ N=M/(1-x) \end{array} \right. = Mx'/x ,$	for $x, x' \in [0, 1]$
$N_{\eta,N}^{(2)}(\eta') \mapsto M_{x,M}^{(2)}(x') := (1 - \eta')N_{\eta,N}^{(2)}(\eta')$	$\left \begin{array}{l} \eta=x, \eta'=x' \\ N=M/(1-x) \end{array} \right. = M - x + x' ,$	
$N_{g,N}^{(1)}(g') \mapsto M_{x,M}^{(1)}(x') := (g' - 1)N_{g,N}^{(1)}(g')$	$\left \begin{array}{l} g=x, g'=x' \\ N=M/(x-1) \end{array} \right. = M ,$	for $x, x' \geq 1$
$N_{g,N}^{(2)}(g') \mapsto M_{x,M}^{(2)}(x') := (g' - 1)N_{g,N}^{(2)}(g')$	$\left \begin{array}{l} g=x, g'=x' \\ N=M/(x-1) \end{array} \right. = (M - 1)x'/x + 1 ,$	
$N_{\eta,N}^{(3)}(g') \mapsto M_{x,M}^{(3)}(x') := (g' - 1)N_{\eta,N}^{(3)}(g')$	$\left \begin{array}{l} \eta=x, g'=x' \\ N=M/(1-x) \end{array} \right. = (M - x)x'/x + 1 ,$	for $x \in [0, 1]$ and $x' \geq 1$
$N_{\eta,N}^{(4)}(g') \mapsto M_{x,M}^{(4)}(x') := (g' - 1)N_{\eta,N}^{(4)}(g')$	$\left \begin{array}{l} \eta=x, g'=x' \\ N=M/(1-x) \end{array} \right. = M + 1 - x ,$	
$N_{g,N}^{(3)}(\eta') \mapsto M_{x,M}^{(3)}(x') := (1 - \eta')N_{g,N}^{(3)}(\eta')$	$\left \begin{array}{l} g=x, \eta'=x' \\ N=M/(x-1) \end{array} \right. = M - 1 + x' ,$	for $x \geq 1$ and $x' \in [0, 1]$
$N_{g,N}^{(4)}(\eta') \mapsto M_{x,M}^{(4)}(x') := (1 - \eta')N_{g,N}^{(4)}(\eta')$	$\left \begin{array}{l} g=x, \eta'=x' \\ N=M/(x-1) \end{array} \right. = (M + x - 1)x'/x ,$	

TABLE II: Border lines of the regions $\mathbb{L}_{x,M}^{(0)}$ of Eq. (78) and $\mathbb{H}_{x,M}^{(0)}$ of Eq. (79) for the $\Phi_{x,M}$ map.

of $\mathbb{L}_{x_2,M_2}^{(0)}$ (indeed $\Phi_{x',M'} = \Phi_{\bar{x}_1,\bar{M}_1} \circ \Phi_{x_2,M_2}$). However, because of Eq. (88) the latter is a subset of $\mathbb{L}_{x,M}^{(0)}$, so we can conclude that

$$(x', M') \in \mathbb{L}_{x,M} \implies (x', M') \in \mathbb{L}_{x,M}^{(0)} , \quad (90)$$

which together with Eq. (42) gives the first of the identities Eq. (87).

By the same token, let $(x', M') \in \mathbb{H}_{x,M}$: from (27) it follows that we can write

$$\Phi_{x,M} = \Phi_{\bar{x}_1,\bar{M}_1} \circ \Phi_{x',M'} \circ \Phi_{\bar{x}_2,\bar{M}_2} , \quad (91)$$

for some proper choice of $(\bar{x}_1, \bar{M}_1), (\bar{x}_2, \bar{M}_2) \in (\mathbb{R}^+)^2$. Setting then $\Phi_{x_2,M_2} := \Phi_{x',M'} \circ \Phi_{\bar{x}_2,\bar{M}_2}$, we can claim that (x', M') is an element of $\mathbb{H}_{x_2,M_2}^{(0)}$, and (x_2, M_2) an element of $\mathbb{H}_{x,M}^{(0)}$ (indeed $\Phi_{x,M} = \Phi_{\bar{x}_1,\bar{M}_1} \circ \Phi_{x_2,M_2}$). However, because of Eq. (88) it follows that $\mathbb{H}_{x_2,M_2}^{(0)}$ is included into $\mathbb{H}_{x,M}^{(0)}$, so that

$$(x', M') \in \mathbb{H}_{x,M} \implies (x', M') \in \mathbb{H}_{x,M}^{(0)} , \quad (92)$$

which gives the second of the identities Eq. (87). \square

C. Three-elements concatenation regions for channels $\Phi_{x,M}$ fulfilling (36)

Here we show that for channels $\Phi_{x,M}$ which are deep in the EB region (i.e. such that (36) holds true), the low-ground/high-ground regions are determined by Eqs. (38) and (37). To begin with let us observe that, for $M \geq$

$M_{\text{EB}}(x)$, Eqs. (81)–(84) lead to express the two-elements concatenation sets $\mathbb{L}_{x,M}^{(0)}$ and $\mathbb{H}_{x,M}^{(0)}$ as

$$\mathbb{L}_{x,M}^{(0)} = \left\{ (x', M') \in (\mathbb{R}^+)^2 : \right. \quad (93)$$

$$\left. M' \geq \min\{f_{x,M}^{(1)}(x'), f_{x,M}^{(2)}(x')\} \right\} ,$$

$$\mathbb{H}_{x,M}^{(0)} = \left\{ (x', M') \in (\mathbb{R}^+)^2 : \right. \quad (94)$$

$$\left. M' \leq \max\{f_{x,M}^{(1)}(x'), f_{x,M}^{(2)}(x')\} \right\} ,$$

with $f_{x,M}^{(1,2)}(x')$ the functions defined in Eq. (33). It turns out that such regions always admit a non trivial overlap $\mathbb{O}_{x,M}^{(0)} := \mathbb{L}_{x,M}^{(0)} \cap \mathbb{H}_{x,M}^{(0)}$ that includes a finite portion of the plane $(\mathbb{R}^+)^2$ in the neighbourhood of the origin – see Fig. 6. As a matter of fact $(0, 0)$ itself can be considered as element of $\mathbb{O}_{x,M}^{(0)}$ (to be precise, it is an element of the closure of $\mathbb{O}_{x,M}^{(0)}$ – see App. B for a refinement of the following argument, taking this into account), i.e.

$$M > M_{\text{EB}}(x) \implies (0, 0) \in \mathbb{O}_{x,M}^{(0)} \subseteq \mathbb{H}_{x,M}^{(0)} \subseteq \mathbb{H}_{x,M} . \quad (95)$$

Now from (26) and (31) we know that

$$(x', M') \in \mathbb{H}_{0,0} , \quad \forall (x', M') \in (\mathbb{R}^+)^2 , \quad (96)$$

which using (29) gives

$$(x', M') \in \mathbb{H}_{x,M} , \quad \forall (x', M') \in (\mathbb{R}^+)^2 , \quad (97)$$

hence proving Eq. (37). Observe next that if (x', M') is also EB, then from (97) we also have $(x, M) \in \mathbb{H}_{x',M'}$ which lead to Eq. (38) via the complementarity rule (31).

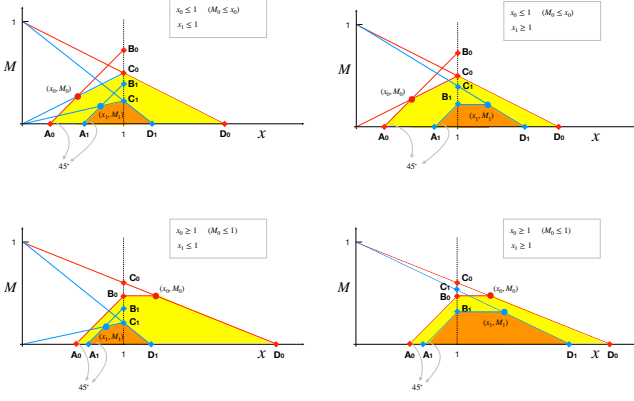


FIG. 5: Graphical explanation of inclusions rules of Eq. (88). The border of the high ground region can have two different shapes, depending on x_i being smaller or larger than 1 (the degenerate case $x_i = 1$ is not plotted but it is analogous). In the case $x_i < 1$, the region is obtained as the intersection of $(\mathbb{R}^+)^2$ with the half-planes delimited by a 45 degrees line passing through (x_i, M_i) , a line passing through the origin and (x_i, M_i) and intersecting the $x = 1$ line at \mathbf{C}_i , and a line passing through \mathbf{C}_i and $(0, 1)$. In the case $x_i > 1$, the region is obtained as the intersection of $(\mathbb{R}^+)^2$ with the half-planes delimited by an horizontal line passing through (x_i, M_i) and intersecting the $x = 1$ line at \mathbf{B}_i , a 45 degrees line intersecting \mathbf{B}_i , and a line passing through (x_i, M_i) and $(0, 1)$. If $x_0 < 1$ and $x_1 < 1$, all the the intersection of $(\mathbb{R}^+)^2$ and the half-planes individuated by the segments $\mathbf{A}_1 - (x, M)$, $(x, M) - \mathbf{C}_1$ and $\mathbf{C}_1 - \mathbf{D}_1$ are contained in the corresponding region individuated by x_0 , and therefore their intersection also satisfy the same inclusions. If $x_0 > 1$ and $x_1 > 1$, all the the intersection of $(\mathbb{R}^+)^2$ and the half-planes individuated by the segments $\mathbf{A}_1 - \mathbf{B}_1$, $\mathbf{B}_1 - (x, M)$, and $(x, M) - \mathbf{D}_1$ are contained in the corresponding region individuated by x_0 , and therefore their intersection also satisfy the same inclusions. If $x_0 < 1$ and $x_1 > 1$, a calculation shows that in the non EB region the region on the left is convex, therefore it contains the triangle $\mathbf{A}_1 - \mathbf{B}_1 - (1, 0)$, while the inclusion of the triangle $\mathbf{C}_1 - \mathbf{D}_1 - (1, 0)$ follows from the same half-plane argument as before. If $x_0 > 1$ and $x_1 < 1$, a calculation shows that in the non EB region the region on the right is convex, therefore it contains the triangle $\mathbf{C}_1 - \mathbf{D}_1 - (1, 0)$, while the inclusion of the triangle $\mathbf{A}_1 - \mathbf{C}_1 - (1, 0)$ follows from the same half-plane argument as before.

VI. STABILIZING BOUNDS

Building up from the low-ground/high-ground analysis presented in the previous sections we can now detail a general technique that allows one to potentially improve existing upper and lower bounds for the capacities of single-mode PI-GBCs. Indeed suppose that $\mathcal{K}^{(+)}(x, M)$, $\mathcal{K}^{(-)}(x, M)$ are two functions which bound for the capacity $\mathcal{K}(x, M) := \mathcal{K}(\Phi_{x, M})$ of the channel $\Phi_{x, M}$, i.e.

$$\mathcal{K}^{(+)}(x, M) \geq \mathcal{K}(x, M) \geq \mathcal{K}^{(-)}(x, M), \quad (98)$$

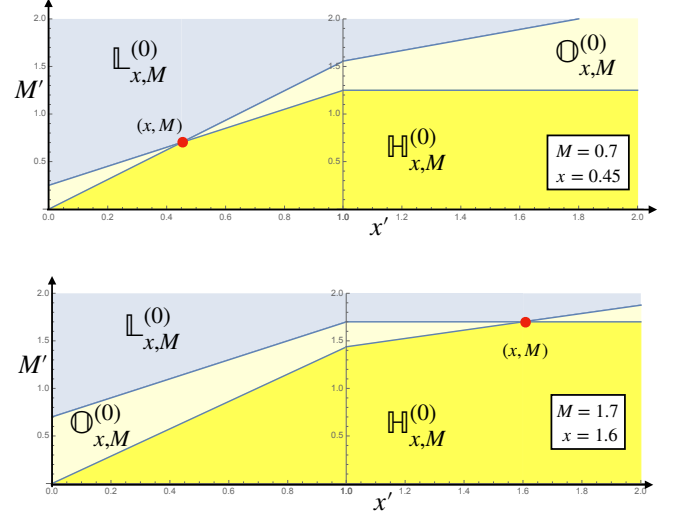


FIG. 6: Examples of the two-elements compositions low-ground/high-ground regions $\mathbb{L}_{x, M}^{(0)}$ and $\mathbb{H}_{x, M}^{(0)}$ for EB channels $\Phi_{x, M}$. Notice that such sets admits a non trivial overlap $\mathbb{O}_{x, M}^{(0)} := \mathbb{L}_{x, M}^{(0)} \cap \mathbb{H}_{x, M}^{(0)}$ (pale yellow region) which always includes the origin point $(0, 0)$.

for all $(x, M) \in (\mathbb{R}^+)^2$. From (25) and (28) it follows that the quantities

$$\begin{cases} \underline{\mathcal{K}}^{(+)}(x, M) &:= \min_{(x', M') \in \mathbb{H}_{x, M}^{(0)}} \mathcal{K}^{(+)}(x', M'), \\ \overline{\mathcal{K}}^{(-)}(x, M) &:= \max_{(x', M') \in \mathbb{L}_{x, M}^{(0)}} \mathcal{K}^{(-)}(x', M'), \end{cases} \quad (99)$$

can potentially improve the inequalities (98), i.e.

$$\begin{cases} \mathcal{K}^{(+)}(x, M) \geq \underline{\mathcal{K}}^{(+)}(x, M), \\ \underline{\mathcal{K}}^{(+)}(x, M) \geq \mathcal{K}(x, M) \geq \overline{\mathcal{K}}^{(-)}(x, M), \\ \overline{\mathcal{K}}^{(-)}(x, M) \geq \mathcal{K}^{(-)}(x, M). \end{cases} \quad (100)$$

Of course it is very possible that the functions $\underline{\mathcal{K}}^{(+)}(x, M)$ and $\overline{\mathcal{K}}^{(-)}(x, M)$ will coincides with $\mathcal{K}^{(+)}(x, M)$ and $\mathcal{K}^{(-)}(x, M)$, respectively: this happens for instance for all bounding functions (98) which arise from operational procedures that automatically incorporate data processing, e.g. the bounds (18), (22), and (23). There are however examples where the construction (99) leads to non trivial overall improvements. In what follow we shall detail one of such cases.

A. Improving the upper bounds for the quantum capacity of thermal attenuators

Expressing the functions (22) in terms of the parametrization (3) we can claim that the quantum and

private capacities of the channel $\Phi_{x,M}$ is always smaller than or equal to

$$Q_{\text{FKG}}(x, M) := \begin{cases} Q_{\text{FKG}}^{\text{att}}(x, \frac{M}{1-x}), & \forall x \in [0, 1], \\ Q_{\text{FKG}}^{\text{amp}}(M), & \forall x \geq 1. \end{cases} \quad (101)$$

Following Eq. (99) we can produce an upper bound $\underline{Q}_{\text{FKG}}(x, M)$ by taking the minimum of $Q_{\text{FKG}}(x', M')$ over the set $\mathbb{H}_{x,M}$. This strategy had been suggested and shown to give improvements in [41], and it will be fully explored here. Without loss of generality we assume (x, M) not to belong to the AD domain \mathbb{A} , i.e.

$$\begin{cases} x \geq 1/2, \\ M \leq M_{\text{AD}}(x) = \min\{x - 1/2, 1/2\}, \end{cases} \quad (102)$$

a condition which via Eq. (35), allows us to identify the high-ground set of the model with the yellow regions of Fig. 3. We next compute the value $\underline{Q}_{\text{FKG}}^{(1)}(x, M)$ which represents the minimum of $Q_{\text{FKG}}(x', M')$ for points of $\mathbb{H}_{x,M}$ which have $x' \in [0, 1]$, and the value $\underline{Q}_{\text{FKG}}^{(2)}(x, M)$ which instead involves points of $\mathbb{H}_{x,M}$ with $x \geq 1$, i.e.

$$\begin{aligned} \underline{Q}_{\text{FKG}}^{(1)}(x, M) &:= \min_{(x', M') \in \mathbb{H}_{x,M}; x' \in [0, 1]} Q_{\text{FKG}}^{\text{att}}(x', \frac{M'}{1-x'}), \\ \underline{Q}_{\text{FKG}}^{(2)}(x, M) &:= \min_{(x', M') \in \mathbb{H}_{x,M}; x' \geq 1} Q_{\text{FKG}}^{\text{amp}}(M'). \end{aligned} \quad (103)$$

Once we have these terms we can then write the global minimum of $Q_{\text{FKG}}(x, M)$ over $\mathbb{H}_{x,M}$ as

$$\underline{Q}_{\text{FKG}}(x, M) = \min\{\underline{Q}_{\text{FKG}}^{(1)}(x, M), \underline{Q}_{\text{FKG}}^{(2)}(x, M)\}. \quad (104)$$

Consider first the evaluation of $\underline{Q}_{\text{FKG}}^{(2)}(x, M)$. Let us start observing that from Eqs. (83) and (84), the maximum value of M' we can get for points (x', M') of $\mathbb{H}_{x,M}$ with $x' \geq 1$ is

$$M_{\text{max}}^{(>)}(x) := \begin{cases} M/x, & \forall x \in [\frac{1}{2}, 1] \\ M, & \forall x \geq 1 \end{cases} = \frac{M}{M_{\text{EB}}(x)}, \quad (105)$$

which, in virtue of Eq. (VII) is always smaller than or equal to $1/2$. Recalling hence that on the interval $\kappa \in [0, 1/2]$ the function $Q_{\text{FKG}}^{\text{amp}}(\kappa)$ is monotonically decreasing, we can write

$$\begin{aligned} \underline{Q}_{\text{FKG}}^{(2)}(x, M) &= Q_{\text{FKG}}^{\text{amp}}(M_{\text{max}}^{(>)}(x)) \\ &= -\log_2\left(\frac{eM}{M_{\text{EB}}(x)}\right) + 2h\left(\frac{\sqrt{M^2 + M_{\text{EB}}^2(x)} - M_{\text{EB}}^2(x)}{2M_{\text{EB}}(x)}\right). \end{aligned} \quad (106)$$

In the case of amplifiers (i.e. for $x \geq 1$) this implies that $\underline{Q}_{\text{FKG}}^{(2)}(x, M)$ always coincides with the old bound (101), so no improvement can be obtained.

Consider next $\underline{Q}_{\text{FKG}}^{(1)}(x, M)$. Here the key observation is that for fixed value of x' , $Q_{\text{FKG}}^{\text{att}}(x', \frac{M'}{1-x'})$ is a decreasing

function of M' . Observe also that for $x \in [\frac{1}{2}, 1]$, Eqs. (81) and (82) implies that the maximum value of M' we can get for points (x', M') of $\mathbb{H}_{x,M}$ which have $x' \leq 1$ is

$$M_{\text{max}}^{(<)}(x', x) := \begin{cases} M + x' - x, & \forall x' \in [x - M, x], \\ \frac{x'}{x}M, & \forall x' \in [x, 1]. \end{cases} \quad (107)$$

Therefore we can write

$$\begin{aligned} \underline{Q}_{\text{FKG}}^{(1)}(x, M) &= \min_{x' \in [x-M, 1]} Q_{\text{FKG}}^{\text{att}}(x', \frac{M_{\text{max}}^{(<)}(x', x)}{1-x'}) \\ &= \min\{\underline{Q}_{\text{FKG}}^{(1.1)}(x, M), \underline{Q}_{\text{FKG}}^{(1.2)}(x, M)\}, \end{aligned} \quad (108)$$

with

$$\begin{aligned} \underline{Q}_{\text{FKG}}^{(1.1)}(x, M) &:= \min_{x' \in [x-M, x]} Q_{\text{FKG}}^{\text{att}}(x', \frac{M+x'-x}{1-x'}) \\ &= \min_{\epsilon \in [0, 1]} Q_{\text{FKG}}^{\text{att}}(x - \epsilon M, \frac{(1-\epsilon)M}{1-x+\epsilon M}), \end{aligned} \quad (109)$$

where the second identify simply follows from a proper parametrization of x' , and

$$\begin{aligned} \underline{Q}_{\text{FKG}}^{(1.2)}(x, M) &:= \min_{x' \in [x, 1]} Q_{\text{FKG}}^{\text{att}}(x', \frac{x'M}{(1-x')x}) \\ &= \min_{\epsilon \in [0, 1]} Q_{\text{FKG}}^{\text{att}}\left(1 + \epsilon(1-x), \frac{1+\epsilon(1-x)M}{(1-x)x\epsilon}\right). \end{aligned} \quad (110)$$

Notice that for $\epsilon = 0$ the function $Q_{\text{FKG}}^{\text{att}}(x - \epsilon M, \frac{(1-\epsilon)M}{1-x+\epsilon M})$ corresponds to $Q_{\text{FKG}}^{\text{att}}(x, M)$ in Eq. (22) while for $\epsilon = 1$ we recover the bound $Q(\mathcal{E}_{x-M, 0})$ of Eq. (20). Therefore for the attenuators we have that $\underline{Q}_{\text{FKG}}^{(1.1)}(x, M)$ (and hence $\underline{Q}_{\text{FKG}}^{(1)}(x, M)$) is always guaranteed to provide bounds which are at least equal than those reported in Eqs. (22) and (20), i.e.

$$\underline{Q}_{\text{FKG}}^{(1)}(x, M) \leq \min\{Q(\mathcal{E}_{x-M, 0}), Q_{\text{FKG}}^{\text{att}}(x, M)\}. \quad (111)$$

On the contrary for $x \geq 1$, Eq. (107) gets replaced

$$M_{\text{max}}^{(<)}(x', x) := M + x' - 1, \forall x' \in [1 - M, 1], \quad (112)$$

leading to

$$\begin{aligned} \underline{Q}_{\text{FKG}}^{(1)}(x, M) &:= \min_{x' \in [1-M, 1]} Q_{\text{FKG}}^{\text{att}}(x', \frac{M+x'-1}{1-x'}) \\ &= \min_{\epsilon \in [0, 1]} Q_{\text{FKG}}^{\text{att}}\left(1 - \epsilon M, \frac{1-\epsilon}{\epsilon}\right). \end{aligned} \quad (113)$$

1. Numerical analysis

Numerical analysis shows that $\underline{Q}_{\text{FKG}}^{(1.2)}(x, M)$ is always less performant than $\underline{Q}_{\text{FKG}}^{(1.1)}(x, M)$ so we can drop it from Eq. (104). Accordingly we can claim that for an attenuator channel ($x \leq 1$) the quantum capacity $Q(\Phi_{x,M})$ must fulfil two new sets of inequalities, i.e.

$$Q(\Phi_{x,M}) \leq \underline{Q}_{\text{FKG}}^{(2)}(x, M) = Q_{\text{FKG}}^{\text{amp}}(M/x), \quad (114)$$

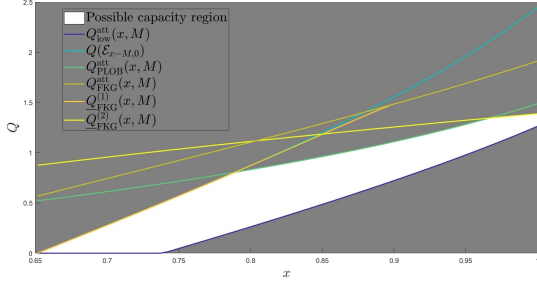


FIG. 7: Comparison between state of the art upper bounds on the quantum capacity $Q(\Phi_{x,M})$ of thermal attenuator ($x \leq 1$) for $M = 0.15$. Each color represents an upper bound on the quantum capacity of thermal attenuator. For $x < 0.78$, the function $Q_{\text{FKG}}^{(1)}(x, M)$ in Eq. (115) is the best upper bound (note that in this region $Q(\mathcal{E}_{\eta-N(1-\eta),0})$ and $Q_{\text{FKG}}^{(1)}(x, M)$ are very close, by numerical evidence). For $x > 0.97$, the function $Q_{\text{FKG}}^{(2)}(x, M)$ in Eq. (114) outperforms the other bounds, and the for intermediate values of x i.e. $0.78 < x < 0.97$, bound $Q_{\text{PLOB}}^{\text{att}}(x, M)$ in Eq. (18) wins. The purple line represents the lower bound $Q_{\text{low}}^{\text{att}}(x, M)$ in Eq. (23), and the white region indicates the possible values of quantum capacity of thermal attenuator.

which follows from (106) and (105), and

$$Q(\Phi_{x,M}) \leq \underline{Q}_{\text{FKG}}^{(1)}(x, M) = \min_{\epsilon \in [0,1]} Q_{\text{FKG}}^{\text{att}}(x - \epsilon M, \frac{(1-\epsilon)M}{1-x+\epsilon M}), \quad (115)$$

which instead follows from (109). As shown in Fig. 7 for some value of the channel parameter these two functions provide better upper bounds than those reported in Sec. III A.

For amplifiers (i.e. $x \geq 1$) we have already observed

that $\underline{Q}_{\text{FKG}}^{(2)}(x, M)$ always coincides with the old bound (101). Accordingly new results can only derive from $\underline{Q}_{\text{FKG}}^{(1)}(x, M)$ (i.e. from $Q_{\text{FKG}}^{(1.1)}(x, M)$): unfortunately numerical study reveals that such function is always less performant than the bounds of Sec. III A. A comprehensive comparison between the old bounds and the improved versions derived in this section is presented in the right part of Fig. 2.

VII. CONCLUSION

In the present manuscript, we sought to better understand the behavior of the capacities of single-mode phase-insensitive Gaussian bosonic channels (PI-GBCs) and their concatenation rules. Through extensive analysis, we were able to establish, for each point in the parameter space of PI-GBCs, an analytical characterization of two regions in the parameter space, of higher and lower capacity. That is, the capacity of points within each region was found to be respectively higher or lower than that of the original channel. Using these regions, we were able to improve upon the previous upper bounds. This structure of parameter phase space of PI-GBCs can be used to potentially improve any new upper or lower bound.

We thank F. A. Mele and L. Lami for comments and suggestions. We also acknowledge financial support by MUR (Ministero dell' Università e della Ricerca) through the PNRR MUR project PE0000023-NQSTI. MF is supported by Juan de la Cierva - Formación (Spanish MICIN project FJC2021-047404-I), with funding from MCIN/AEI/10.13039/501100011033 and European Union "NextGenerationEU"/PRTR.

-
- [1] C. E. A Shannon, Bell Syst. Tech. J. **27**, 379–423 (1948)
 - [2] C. E. A Shannon, Bell Syst. Tech. J. **27**, 623–656 (1948)
 - [3] C. H. Bennett and P. W. Shor, IEEE Trans. Inf. Th. **44**, 2724–2742, (1998).
 - [4] V. Giovannetti and H.S. Holevo Rep. Prog. Phys. **75** 046001 (2012).
 - [5] A. S. Holevo, *Quantum systems, channels, information: a mathematical introduction* (de Gruyter, 2012).
 - [6] M. Wilde, *Quantum Information Theory* (Cambridge University Press, 2013).
 - [7] C. M. Caves and P. D. Drummond Rev. Mod. Phys. **66**, 481 (1994).
 - [8] A. S. Holevo and R. F. Werner, Phys. Rev. A, **63** 032312, (2001).
 - [9] A. Serafini, *Quantum Continuous Variables: A Primer of Theoretical Methods* (CRC Press, London, 2017).
 - [10] J. S. Sidhu *et al.* IET Quantum Communication, **2**:182, (2021).
 - [11] P. Shor, *The quantum channel capacity and coherent information*. Lecture notes, MSRI Workshop on Quantum Computation (2002).
 - [12] S. Lloyd, Phys. Rev. A **55**, 1613 (1997).
 - [13] I. Devetak, IEEE Trans. Inf. Th. **51**, 44 (2005).
 - [14] N. Cai, A. Winter, and R. W. Yeung, Problems of Information Transmission **40**, 318 (2004).
 - [15] I. Devetak and P. W. Shor, Commun. Math. Phys. **256**, 287 (2015)
 - [16] P. W. Shor, and J. A. Smolin, arXiv preprint quant-ph/9604006 (1996).
 - [17] D. P. DiVincenzo, P. W. Shor, and J. A. Smolin, Phys. Rev. A **57**, 830 (1998).
 - [18] G. Smith and J. A. Smolin, Phys. Rev. Lett. **98**, 030501 (2007).
 - [19] J. Fern and K. B. Whaley, Phys. Rev. A **78**, 062335 (2008).
 - [20] G. Smith and J. Yard. Science **321**, 1812 (2008).
 - [21] G. Smith, J. Smolin, and J. Yard. Nat. Phot. **5**, 624 (2011).
 - [22] T. Cubitt, D. Elkouss, W. Matthews, M. Ozols, D. Pérez-García, and S. Strelchuk, Nat. Comm. **6**, 1 (2015).
 - [23] F. Leditzky, D. Leung, and G. Smith, Phys. Rev. Lett. **121**, 160501 (2018).

- [24] J. Bausch and F. Leditzky, *SIAM J. Comput.* **50** 1410 (2021)
- [25] M. Hastings, *Nat. Phys.* **5**, 255 (2009).
- [26] K. Li, A. Winter, X. B. Zou, and G. C. Guo, *Phys. Rev. Lett.* **103**, 120501 (2009).
- [27] E. Y. Zhu, Q. Zhang and P. W. Shor, *Phys. Rev. Lett.* **119**, 040503 (2017).
- [28] E. Y. Zhu, Q. Zhang, M-H Hsieh, and P. W. Shor, *IEEE Trans. Inf. Th.* **65**, 3973 (2018).
- [29] V. Siddhu, *Nat. Comm.* **12**, 5750 (2021).
- [30] G. Smith and J. A. Smolin, *IEEE Information Theory Workshop*, vol. **54**, 4208 (2008).
- [31] Y. Ouyang, *Quantum Information & Computation* **14**, 917 (2014).
- [32] D. Sutter, V. B. Scholz, A. Winter, and R. Renner, *IEEE Trans. Inf. Th.* **63**, 7832 (2017).
- [33] F. Leditzky, D. Leung, and G. Smith, *Phys. Rev. Lett.* **120**, 160503 (2018).
- [34] F. Leditzky, N. Datta, and G. Smith, *IEEE Trans. Inf. Th.* **64** 4689 (2018).
- [35] M. Fanizza, F. Kianvash, and V. Giovannetti, *Phys. Rev. Lett.* **125**, 020503 (2020).
- [36] F. Kianvash, M. Fanizza, and V. Giovannetti, *Quantum* **6**, 647 (2022)
- [37] X. Wang, *IEEE Trans. Inf. Th.* **67**, 4524 (2021).
- [38] K. Sharma, M. M. Wilde, S. Adhikari & M. Takeoka, *New J. Phys.* **20**, 063025 (2018).
- [39] K. Noh, V.V. Albert, and L. Jiang, *IEEE Trans. Inf. Th.* **65**, 2563 (2018).
- [40] M. Rosati, A. Mari, and V. Giovannetti, *Nat. Comm.* **9**, 4339 (2018)
- [41] M. Fanizza, F. Kianvash, and V. Giovannetti, *Phys. Rev. Lett.* **127**, 210501 (2021).
- [42] S. Pirandola, R. Laurenza, C. Ottaviani, and L. Banchi, *Nat. Comm.* **8**, 15043 (2017).
- [43] I. Devetak and P. W. Shor, *Comm. Math. Phys.* **256**, 2 (2005).
- [44] C. H. Bennett, P. W. Shor, J. A. Smolin, and A. V. Thapliyal, *Phys. Rev. Lett.* **83**, 3081 (1999).
- [45] F. A. Mele, L. Lami, and V. Giovannetti, *arXiv:2303.12867* [quant-ph].
- [46] L. Lami, S. Khatir, G. Adesso, and M. M. Wilde, *Phys. Rev. Lett.* **123**, 050501 (2019).
- [47] F. Caruso, and V. Giovannetti, *Physical Review A* **74**, 062307 (2006).
- [48] F. Caruso, V. Giovannetti, and A S Holevo, *New Journal of Physics* **8**, 310 (2006).
- [49] A. S. Holevo, *Problems of Information Transmission* **43**, 1 (2007).
- [50] M. M. Wolf, D. Perez-Garcia, G. Giedke, *Phys. Rev. Lett.* **98**, 130501 (2007).
- [51] M.M. Wilde, M. Tomamichel, and M. Berta, *IEEE Trans. Inf. Th.* **63**, 1792 (2017).
- [52] S. Pirandola, R. Garcia-Patron, S. L. Braunstein, and S. Lloyd, *Phys. Rev. Lett.* **102** 050503 (2009).
- [53] C. Ottaviani, R. Laurenza, T.P. Cope, G. Spedalieri, S.L. Braunstein, and S. Pirandola, October. *Quantum Information Science and Technology II SPIE* **9966**, 16 (2016)
- [54] Notice that, thanks to (5), the definition (24) includes also all those cases where $\Phi_{x',M'}$ and $\Phi_{x,M}$ are connected with more complex decompositions that involve more than one left-most or on the right-most elements. For instance $\Phi_{x',M'} = \left(\Phi_{\bar{x}_{1,1},\bar{M}_{1,1}} \circ \Phi_{\bar{x}_{1,2},\bar{M}_{1,2}} \right) \circ \Phi_{x,M} \circ \Phi_{\bar{x}_2,\bar{M}_2}$

can be casted into the form $\Phi_{x',M'} = \Phi_{\bar{x}_1,\bar{M}_1} \circ \Phi_{x,M} \circ \Phi_{\bar{x}_2,\bar{M}_2}$ by simply identifying $\Phi_{\bar{x}_1,\bar{M}_1}$ with $\Phi_{\bar{x}_{1,1},\bar{M}_{1,1}} \circ \Phi_{\bar{x}_{1,2},\bar{M}_{1,2}}$. Similar considerations of course apply also to Eq. (27).

- [55] In writing (38) we used the fact that that $f_{0,0}^{(1)}(x') = \min\{1, x'\}$, and that the proper limit $x \rightarrow 0, M \rightarrow 0$ of $f_{x,M}^{(2)}(x')$ is given by $f_{0,0}^{(2)}(x') = -(x' - 1)\Theta(x' - 1)$.

Appendix A: Monotonicity along the borders

Notice that as the property (50) imposes in particular that $\mathcal{K}(\mathcal{E}_{\eta,N}) \geq \mathcal{K}(\mathcal{E}_{\eta',N'})$ for all $\eta' \leq \eta$, $N' \geq N$, it follows that $\mathcal{K}(\mathcal{E}_{\eta,N})$ must be non-decreasing in η for fixed N , and non-increasing w.r.t. N for fixed η . Similarly, from (64) it follows that $\mathcal{K}(\mathcal{A}_{g,N})$ must be non-increasing in g for fixed N , and non-increasing w.r.t. N for fixed g .

More generally we can establish the following monotonicity rules for points that lies along the borders of the low-ground/high-ground regions, i.e.

Corollary 4.2. *The capacity \mathcal{K} of the channel $\mathcal{E}_{\eta',N'}$ as a function of η' is monotonically non-decreasing when evaluated along points of the curve $N' = N_{\eta,N}^{(1)}(\eta')$, and monotonically non-increasing when evaluated along points of the curve $N' = N_{\eta,N}^{(2)}(\eta')$. Analogously the capacity \mathcal{K} of the channel $\mathcal{A}_{g',N'}$ as a function of g' is monotonically non-increasing when evaluated along points of the curve $N' = N_{g,N}^{(1)}(g')$, and monotonically non-decreasing when evaluated along points of the curve $N' = N_{g,N}^{(2)}(g')$.*

(It goes without mentioning that, in the case of $N_{\eta,N}^{(2)}(\eta')$ and $N_{g,N}^{(2)}(g')$ the above properties apply only for those points where these functions are explicitly non negative).

Proof. We report here only the proof for the attenuator, as the one for the amplifiers can be obtained by following the same steps. Let us start addressing the monotonicity along the curve $N' = N_{\eta,N}^{(1)}(\eta')$. If $\eta'_1 \leq \eta'_2$ and $N'_1 = N_{\eta,N}^{(1)}(\eta'_1)$, $N'_2 = N_{\eta,N}^{(1)}(\eta'_2)$, we can write

$$\begin{aligned} N_{\eta'_2,N'_2}^{(1)}(\eta'_1) &= \left(\frac{1-\eta'_2}{\eta'_2}\right)N'_2\left(\frac{\eta'_1}{1-\eta'_1}\right) = \left(\frac{1-\eta}{\eta}\right)N\left(\frac{\eta'_1}{1-\eta'_1}\right) \\ &= N_{\eta,N}^{(1)}(\eta'_1) = N'_1. \end{aligned} \quad (\text{A1})$$

Therefore we can conclude that $(\eta'_1, N'_1) \in \mathbb{L}_{\eta'_2,N'_2}^{(\text{att})}$ which implies $\mathcal{K}(\mathcal{E}_{\eta'_1,N'_1}) \leq \mathcal{K}(\mathcal{E}_{\eta'_2,N'_2})$ as a direct consequence of (47) of Property 1. Consider next the monotonicity along the curve $N' = N_{\eta,N}^{(2)}(\eta')$ for points η' for which $N_{\eta,N}^{(2)}(\eta')$ is strictly positive. Given then $\eta'_1 \leq \eta'_2$ values that fulfils such constraint can write

$$\begin{aligned} N_{\eta'_1,N'_1}^{(2)}(\eta'_2) &= (N'_1 + 1) \left(\frac{1-\eta'_1}{1-\eta'_2}\right) - 1 \\ &= (N + 1) \left(\frac{1-\eta}{1-\eta_2}\right) - 1 \\ &= N_{\eta,N}^{(2)}(\eta'_2) = N'_2. \end{aligned} \quad (\text{A2})$$

The identity (A2) implies that $(\eta'_2, N'_2) \in \mathbb{L}_{\eta'_1,N'_1}^{(\text{att})}$ that finally leads to $\mathcal{K}(\mathcal{E}_{\eta'_1,N'_1}) \geq \mathcal{K}(\mathcal{E}_{\eta'_2,N'_2})$. \square

The above results also allow us to establish monotonicity rules for the curves $N_{\eta,N}^{(3,4)}(g)$ and $N_{g,N}^{(3,4)}(\eta)$:

Corollary 4.3. *The capacity \mathcal{K} of the channel $\mathcal{E}_{\eta',N'}$ as a function of η' is monotonically non-decreasing when evaluated along points of the curve $N' = N_{g,N}^{(4)}(\eta')$, and monotonically non-increasing when evaluated along points of the curve $N' = N_{g,N}^{(3)}(\eta')$. Analogously the capacity \mathcal{K} of the channel $\mathcal{A}_{g',N'}$ as a function of g' is monotonically non-increasing when evaluated along points of the curve $N' = N_{\eta,N}^{(4)}(g')$, and monotonically non-decreasing when evaluated along points of the curve $N' = N_{\eta,N}^{(3)}(g')$.*

Proof. The derivation relies on the fact that we can map the curves $N_{g,N}^{(3,4)}(\eta')$ and $N_{\eta,N}^{(3,4)}(g')$ into $N_{\eta,N}^{(1,2)}(\eta')$ and $N_{g,N}^{(1,2)}(g')$ respectively. We give here direct proof of this fact only for $N_{\eta,N}^{(4)}(\eta')$: the generalization to the other cases follows trivially. Consider a point (η_1, N_1) on $N_{g,N}^{(4)}(\eta')$: inverting the identity $N_1 = N_{g,N}^{(4)}(\eta_1)$ can write

$$(N + 1) \left(\frac{g-1}{g}\right) = N_1 \left(\frac{1-\eta_1}{\eta_1}\right), \quad (\text{A3})$$

which gives

$$\begin{aligned} N_{g,N}^{(4)}(\eta') &= (N + 1) \left(\frac{g-1}{g}\right) \left(\frac{\eta'}{1-\eta'}\right) \\ &= N_1 \left(\frac{1-\eta_1}{\eta_1}\right) \left(\frac{\eta'}{1-\eta'}\right) = N_{\eta_1,N_1}^{(1)}(\eta'). \end{aligned} \quad (\text{A4})$$

Invoking hence Corollary 4.2 we can now claim that $\mathcal{K}(\mathcal{E}_{\eta', N'})$ will be non-decreasing w.r.t. to η' , hence proving the thesis. \square

Appendix B: Formal derivation of Eq. (97)

The derivation of Eq. (97) presented in the main text suffers from a problem related with the fact that, technically speaking, Eq. (95) is true only in an approximate sense. Indeed from (6) it is clear that any composition involving the channel $\Phi_{0,0}$ is bound to produce only elements with $x = 0$, i.e.

$$\Phi_{\bar{x}_2, \bar{M}_2} \circ \Phi_{0,0} \circ \Phi_{\bar{x}_1, \bar{M}_1} = \Phi_{0, \bar{M}_2 + \Theta(\bar{x}_2 - 1)} . \quad (\text{B1})$$

Therefore as soon as $x > 0$ there is no hope to see $(0,0)$ as an element of its high-ground set $\mathbb{H}_{x,M}$. The way one should interpret Eq. (95) is that for all (x, M) such that (36) holds true then we can find a set of points arbitrarily close to $(0,0)$ which belong to $\mathbb{H}_{x,M}^{(0)}$ and hence into $\mathbb{H}_{x,M}$. To see that this is enough to prove Eq. (97) observe that according to Eq. (83) and (84), for $x' \in]0, \min\{x, 1\}]$ the conditions under which (x', M') can be included into $\mathbb{H}_{x,M}^{(0)}$ (and hence into $\mathbb{H}_{x,M}$) can be expressed as

$$0 \leq M' \leq M + x' - \min\{x, 1\} , \quad (\text{B2})$$

a region which is not empty if (36) holds true. Observe also that according to Eqs. (81) and (82), for all $(x_1, M_1) \in (\mathbb{R}^+)^2$, the points (x', M') such that

$$M' \geq (M_1 + (x_1 - 1)\Theta(x_1 - 1))x'/x_1 , \quad x' \in [0, \min\{x_1, 1\}] , \quad (\text{B3})$$

are always included into $\mathbb{L}_{x_1, M_1}^{(0)}$ (and hence into \mathbb{L}_{x_1, M_1}). Taking then (x, M) EB with $x > M_{\text{EB}}(x)$, and (x_1, M_1) generic, we notice that for all $x'' \in]0, \min\{x_1, 1\}]$ and $M'' := (M_1 + (x_1 - 1)\Theta(x_1 - 1))x''/x_1$ the point (x', \bar{M}') fulfils both Eq. (B2) and (B3). Therefore we can write

$$\left. \begin{array}{l} (x'', M'') \in \mathbb{H}_{x, M} , \\ (x'', M'') \in \mathbb{L}_{x_1, M_1} \implies (x_1, M_1) \in \mathbb{H}_{x'', M''} , \end{array} \right\} \implies (x_1, M_1) \in \mathbb{H}_{x, M} , \quad (\text{B4})$$

where the first implication is a consequence of the complementary relation (31), and the second of the natural ordering (29).